EJAR

Modeling of adsorption isotherms of Methylene Blue onto rice husk activated carbon

Ahmed El Nemr*, Amany El-Sikaily and Azza Khaled

Department of Pollution, Environmental Division, National Institute of Oceanography and Fisheries, Kayet Bey, El-Anfoushy, Alexandria, Egypt
**Corresponding author E-mail: ahmedmoustafaelnemr@yahoo.com, Tel. & Fax: +2035740944*

Received 31st October, 2010; accepted 20th November, 2010

Abstract

The potential use of rice husk carbon (RHC) to remove Methylene blue dye (MB) from artificial wastewater is investigated. The influence of different system variables, adsorbent dosage, initial dye concentration, pH and contact time were studied. Most of known adsorption isotherm models are investigated to study the removal of MB from aqueous solutions by RHC. The error functions equations are applied to the isotherm models results in order to find the best fit isotherm model. This showed that most of the studied isotherm models are applicable to the adsorption of MB by RHC and the best fit models are linear-Langmuir, Kobel-Corrigan and Tempkin isotherm models. The study of RHC concentrations shows that as the amount of the RHC increase, the percentage of MB removal increase accordingly. Optimum pH value for dye adsorption was determined as ~ 7.1. The maximum adsorption capacity obtained from non-linear solving of Langmuir is 370.71 mg/g and. Furthermore, adsorption kinetics of MB onto RHC was studied and the rate of adsorption found to conform to pseudo-second-order kinetics with a good correlation ($R^2 > 0.99$) with intraparticle diffusion as one of the rate determining steps. This study indicates that the activated carbon developed from rice husk may be attractive way for dye removal from its aqueous solution.

Keywords: Rice husk; activated carbon; Methylene blue; adsorption; simulated wastewater.

1. Introduction

Activated carbon is the most important adsorbent with a large surface area and high porosity. Adsorption of organic pollutants from the liquid phase is an important application of activated carbons, which covers a wide range of systems such as drinking water and wastewater treatments, and applications in the food, beverage, pharmaceutical and chemical industries. Activated carbon adsorption has been cited by the US Environmental Protection Agency (EPA) as one of the best available environmental control technologies (Hamdaoui *et al*., 2005).

Rice, a common food of the Egyptian people, is grown throughout Egypt and the production in Egypt is about 9.0 million tons per year. A great amount of rice husk (one-fifth by weight of rice grain production) is also produced every year in the process of rice threshing. In developing countries, the most common disposal method of rice husks is still incineration and dumping outdoors. Air pollution is produced by the ash, fumes, and toxic organic gases produced by the incineration of rice husks. In Egypt, such incineration is now prohibited in rice fields. A certain amount of rice husk waste in Egypt is recycled in agricultural and livestock farms, but most is treated as agricultural waste. The recycling methodology of rice husks related to the adsorption of liquid phases has been previously studied. The rice husk composition is: 32% cellulose, 21% hemicelluloses, 21% lignin, 1.8% extractives, 8% water and 15% mineral ash (Nakbanpote *et al*., 2000). However, the reported composition of rice husk differs widely, as affected by paddy type and climate (Govindararo, 1980). The adsorption of lutein (Proctor and Palaniappans, 1989) and free fatty acids (Proctor and Palaniappans, 1990) from crude soy oil using inorganic ash prepared by the combustion of rice husks has been investigated. The rice husk was used for adsorption of safranin (Vasanth Kumar and Sivanesan, 2007), methylene blue (Vadivelan and Vasanth Kumar, 2005) and direct dye (Abdelwahab *et al*., 2005). The inorganic ash described in the above documents consists exclusively of SiO_2. The adsorption properties of activated rice husks in adsorbing harmful heavy metals in water have also been reported (Ajmal *et al*., 2003; Bishnoi *et al*., 2004).

Methylene blue (MB) is not strongly hazardous, but it can cause some harmful effects. Adsorption of MB from the aqueous phase is a useful tool for product control of adsorbents and used as a pass test for activated carbon product in industry. The objective of the present study was to explore the feasibility of using rice husk to produce new activated carbon, as an adsorbent for dye removal such as MB, a widely used dye in the textile processing industry. The effect of

operating parameters such as solution pH, dye initial concentration, sorbent mass on the adsorptive capacity of the adsorbent was examined. Kinetic studies were conducted to determine the adsorption mechanism. Because of adsorption equilibrium information is the most important piece of information in understanding of an adsorption process, which is well-established technique for the removal of low concentrations of inorganic and organic pollutants, wastewater, and aqueous solutions, the experimental equilibrium data were analyzed in this paper using thirteen adsorption isotherm models with two, three, four and five parameters.

2. Materials and methods

2.1. Biomass

Rice husk was obtained from local rice mills and was washed several times with distilled water followed by filtration. The washed rice husk was oven dried at 150°C for 1 hr (Abdelwahab *et al*., 2005).

2.2. Preparation of Activated carbon from rice husk (RHC)

The dried rice husk biomass 1.0 kg was added in small portion to 1000 ml of 98% H_2SO_4 during 1 h and the resulting reaction mixture was kept overnight at room temperature followed by refluxing for 3 hours in an efficient fume hood. After cooling to room temperature, the reaction mixture was poured onto cold water (3 liters) and filtered. The resulting material was heated in an open oven at 100°C for 1 hr and then soaked in 1% $NaHCO_3$ solution overnight to remove any remaining acid. The obtained carbon was then washed with distilled water until pH of the activated carbon reached 6, dried in an oven at 200°C for 1 hr in the absence of oxygen and sieved to the particle size ≤ 0.063 mm to give 355 g (35.5% yield of the rice husk) and kept in a glass bottle until used (El-Sikaily *et al*., 2006a; El Nemr *et al*., 2007).

2.3. Preparation of synthetic solution

Methylene Blue (MB) (cationic dye, C.I. 52015, $C_{16}H_{18}N_3SCl$) was purchased from Merck, and it was used as received without further purification. The structure of the dye containing a secondary amine group is presented in Figure 1. A stock solution of 1.0 g/L was prepared by dissolving the appropriate amount of MB in 100 ml and completed to 1000 ml with distilled water. Different concentrations ranged between 5 and 75 mg/L of MB were prepared from the stock solution and used as a standard curve. All the chemicals used throughout this study were of analytical-grade reagents. Double-distilled water was used for preparing all of the solutions and reagents. The initial pH is adjusted with 0.1M HCl or 0.1M NaOH. All the adsorption experiments were carried out at room temperature (25±2°C).

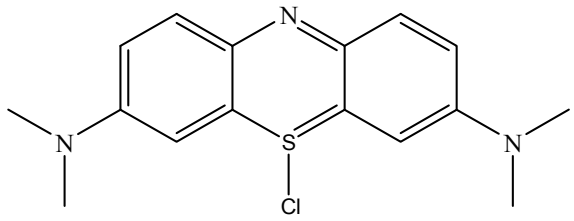

Figure 1. Chemical structure Methylene blue (MB), C.I. 52015, Empirical formula $C_{16}H_{18}N_3SCl$

2.4. Batch biosorption studies

2.4.1. Effect of pH on MB adsorption

The effect of pH on the equilibrium uptake of MB was investigated by employing 75 mg/L initial concentration of MB and RHC 0.5 g/100 ml. The initial pH values were adjusted with 0.1M HCl or 0.1M NaOH to form a series of pH from 1 to 12. The suspensions were shaken at room temperature (25±2°C) using agitation speed (200 rpm) for the minimum contact time required to reach the equilibrium (180 min), then the amount of MB adsorbed was determined (El-Sikaily *et al*., 2006b).

2.4.2. Effect of RHC dose

The effect of sorbents dose on the equilibrium uptake of MB (25, 50, 75, 100 and 125 mg/L) were investigated with RHC concentrations of 1, 2, 4, 5 and 6 g/L. The experiments were performed by shaking known MB initial concentration with the above different RHC concentrations to the equilibrium uptake (180 min) and the amount of MB adsorbed was determined.

2.4.3. Kinetics studies

Adsorption studies were conducted in 500 ml conical flasks at solution of pH 1.0. RHC (0.1, 0.2, 0.3, 0.4, 0.5 and 0.6 g) was thoroughly mixed individually with 100 ml of MB solution of 25, 50, 75, 100 and 125 mg/L concentrations and the suspensions were shaken at room temperature. Samples of 1.0 ml were collected from the duplicate flasks at required time intervals viz. 5, 10, 20, 30, 45, 60, 90, 120, 150 and 180 min and were centrifuged for 5 min. The clear solutions were analyzed for residual MB concentration in the solution.

2.4.4. Adsorption isotherm

Batch adsorption experiments were carried out in 300 ml conical flasks at room temperature on a shaker for 180 min. The RHC (0.1, 0.2, 0.3, 0.4, 0.5 and 0.6 g)

was thoroughly mixed with 100 ml of MB solutions. The isotherm studies were performed by varying the initial MB concentrations from 25 to 125 mg/L at pH 1.0, which was adjusted using 0.1M HCl or 0.1M NaOH before addition of RHC and maintained throughout the experiment. After shaking the flasks for 180 min, the reaction mixture was analyzed for the residual MB concentration.

The concentration of MB in solution was measured by using UV-Visible spectrophotometeric method using UV-VIS spectrophotometer (Milton Roy, Spectronic 21D) using silica cells of path length 1 cm at wavelength λ 665 nm, and MB concentration was determined by comparing absorbance to a calibration curve mentioned above. All the experiments are duplicated and only the mean values are reported. The maximum deviation observed was lesser than ±5%.

The amounts of MB adsorbed at equilibrium (q_e) (mg/g) were calculated from subtracting final solution concentrations from the initial concentration of aqueous solution. The q_e was calculated by the following mass balance relationship:

$$q_e = (C_0 - C_e) \times \frac{V}{W} \quad (1)$$

where C_0 and C_e are the initial and equilibrium liquid-phase concentrations of MB, respectively (mg/L), V the volume of the solution (L), and W is the weight of the MB used (g).

3. Theoretical background

3.1. Two-parameter isotherm models

3.1.1. Langmuir model

The Langmuir model (Langmuir, 1916) assumes uniform energies of adsorption of a solute from a liquid solution onto a surface containing a definite number of identical sites as a monolayer adsorption and no transmigration of adsorbate in the plane of the surface (Doğan *et al*., 2000). Therefore, the Langmuir isotherm model was chosen for estimation of the maximum adsorption capacity corresponding to complete monolayer coverage on the sorbent surface. The Langmuir non-linear equation may be written as equation (2):

$$q_e = \frac{Q_m K_a C_e}{1 + K_a C_e} \quad (2)$$

where, Q_m is a constant reflect a complete monolayer (mg/g); K_a is adsorption equilibrium constant (L/mg) that is related to the apparent energy of sorption. The Langmuir equation (2) can be linearized as shown in equation (3), which gives different ways for parameter estimation (Kinniburgh, 1986; Longhinotti, 1998).

$$\frac{C_e}{q_e} = \frac{1}{K_a Q_m} + \frac{1}{Q_m} \times C_e \quad (3)$$

3.1.2. Freundlich model

The Freundlich model (Freundlich, 1906) is the earliest known equation describing the adsorption process and can be written as equation (4):

$$q_e = K_F C_e^{1/n} \quad (4)$$

where, K_F is a constant indicative of the relative adsorption capacity of the adsorbent and *1/n* is a constant indicative of the intensity of the adsorption of dye onto the sorbent or surface heterogeneity, becoming more heterogeneous as its value gets closer to zero. The Freundlich expression is an exponential equation and therefore, assumes that as the adsorbate concentration increases, the concentration of adsorbate on the adsorbent surface also increases. A value for *1/n* below one indicates a normal Langmuir isotherm while *1/n* above one is indicative of cooperative adsorption. The linear form of the Freundlich isotherm is shown in equation (5):

$$\log q_e = \log K_F + \frac{1}{n} \log C_e \quad (5)$$

To determine the maximum adsorption capacity, it is necessary to operate with constant initial concentration C_0 and variable weights of adsorbent; thus ln Q_m is the extrapolated value of ln q for $C = C_0$. According to Halsey (Halsey, 1952) equation (6):

$$Q_m = K_F C_0^{1/n} \quad (6)$$

where C_0 is the initial concentration of the solute in the bulk solution (mg/L) and Q_m is the Freundlich maximum adsorption capacity (mg/g).

3.1.3. Tempkin model

The Tempkin isotherm model (Tempkin, 1940) assumed that the heat of adsorption of all the molecules in the layer decreases linearly with coverage due to adsorbent-adsorbate interactions, and that the adsorption is characterized by a uniform distribution of the binding energies, up to some maximum binding energy (Kavitha and Namasivayam, 2007). The Tempkin isotherm has commonly been applied in the following form equation (7) (Aharoni and Ungarish, 1977; Aharoni and Sparks, 1991; Wang and Qin, 2005):

$$q_e = \frac{RT}{b}\ln(AC_e) \quad (7)$$

The Tempkin isotherm equation (7) can be simplified to the following equation (8):

$$q_e = \beta \ln A + \beta \ln C_e \quad (8)$$

where $\beta = (RT)/b$, T is the absolute temperature in *Kelvin* and R is the universal gas constant, 8.314 J/mol K. The constant b is related to the heat of adsorption (Pearce *et al*., 2003; Akkaya, A. Ozer, 2005).

3.1.4. The Dubinin-Radushkevich (D-R) model

The Dubinin-Radushkevich (D-R) model (Radushkevich, 1949; Dubinin, 1960; 1965) estimates the porosity apparent free energy and the characteristic of adsorption. The D-R isotherm dose not assumes a homogeneous surface or constant sorption potential. The D-R model has commonly been applied in the following form equation (9) and its linear form can be shown in equation (10):

$$q_e = Q_m \exp(-K\varepsilon^2) \quad (9)$$

$$\ln q_e = \ln Q_m - K\varepsilon^2 \quad (10)$$

where K is a constant related to the adsorption energy, Q_m the theoretical saturation capacity, ε is the Polanyi potential, calculated from equation (11).

$$\varepsilon = RT\ln(1+\frac{1}{C_e}) \quad (11)$$

The slope of the plot of ln q_e versus ε^2 gives K (mol^2 (kJ^2)$^{-1}$) and the intercept yields the adsorption capacity, Q_m (mg/g). The mean free energy of adsorption (E), defined as the free energy change when one mole of ion is transferred from infinity in solution to the surface of the solid, was calculated from the K value using the following relation equation (12) (Kundu and Gupta, 2006):

$$E = 1/\sqrt{(2K)} \quad (12)$$

3.1.5. The Harkins-Jura (HJ) model

The HJ model (Harkins and Jura, 1944) accounts for multilayer adsorption and also for the existence of heterogeneous pore distribution in the adsorbent. The HJ isotherm has commonly been applied in the following form equation (13)

$$\frac{1}{q_e^2} = (\frac{B_{HJ}}{A_{HJ}}) - (\frac{1}{A_{HJ}})\log C_e \quad (13)$$

where A_{HJ} and B_{HJ} are isotherm constant, multilayer adsorption heterogeneous pore distribution.

3.1.6. The Halsey model

Halsey isotherm model (Halsey, 1948) is suitable for multilayer adsorption and the fitting of Halsey equation can be heteroporous solids (Rosen, 1978). The Halsey model has commonly been applied in the following form equation (14):

$$\ln q_e = [(\frac{1}{n_H})\ln K_H] + (\frac{1}{n_H})\ln C_e \quad (14)$$

where n_H and K_H are Halsey constants.

3.1.7. The Henderson model

Henderson isotherm model (Henderson, 1952) is another equation suitable for multilayer adsorption and the fitting of Henderson equation can be heteroporous solids (Rosen, 1978). The Henderson model has commonly been applied in the following form equation (15):

$$\ln[-\ln(1-C_e)] = \ln K_h + (\frac{1}{n_h})\ln q_e \quad (15)$$

where n_h and K_h are Henderson constants.

3.1.8. The Smith model

Also Smith model (Smith, 1947) is suitable for multilayer adsorption. Especially, the fitting of Smith equations can be seen in heteroporous solids (Ertugay *et al*., 2000). The Smith model has commonly been applied in the following form equation (16):

$$q_e = W_{bS} - W_S \ln(1-C_e) \quad (16)$$

where W_{bs} and W_s are the Smith model parameters

3.1.9. Generalized isotherm equation

A linear form of the generalized isotherm equation (Kargi and Ozmichi, 2004; Ozmihci and Kargi, 2006; Kargi and Cikla, 2006) is given by equation (17):

$$\ln[\frac{Q_m}{q_e} - 1] = \ln K_G - N_G \ln Ce \quad (17)$$

where, K_G is the saturation constant (mg/L); N_G the cooperative binding constant; Q_m the maximum adsorption capacity of the adsorbent (mg/g) (obtained from Langmuir model); q_e (mg/g) and C_e (mg/L) are the equilibrium dye concentrations in the solid and liquid phases, respectively. A plot of $\ln[(Q_m/q_e - 1)]$ versus $\ln C_e$; the intercept gave $\log K_G$ and the slope gave N_b constants. Parameters related to each isotherm were determined by using linear regression analysis and the square of the correlation coefficients (R^2) have been calculated.

3.2. Three-parameter isotherm models

3.2.1. Koble-Corrigan isotherm model

Koble-Corrigan model is another isotherm empirical model depends on the combination of the Langmuir and Freundlich isotherm equations in one non-linear equation for representing the equilibrium adsorption data. It is commonly expressed by equation (18) (Costa *et al*., 1986):

$$q_e = \frac{aC_e^n}{1 + bC_e^n} \tag{18}$$

where *a*, *b* and *n* are the Koble-Corrigan parameters.

3.2.2. Redlich-Peterson model

The Redlich-Peterson model (equation 19) (Redlich and Peterson, 1959) isotherm is an empirical isotherm incorporating three parameters. It combines elements from both the Langmuir and Freundlich equations, and the mechanism of adsorption is a hybrid and does not follow ideal monolayer adsorption:

$$q_e = \frac{AC_e}{1 + BC_e^g} \tag{19}$$

where A is the Redlich-Peterson isotherm constant (L/g), B is also a constant having unit of $(L/mg)^{\beta}$, and β is an exponent that lies between 0 and 1.

At high liquid-phase concentrations of the adsorbate, Eq. (19) reduces to the Freundlich model equation (4). At $\beta = 1$, equation (19) reduces to the Langmuir model equation (2) and at $\beta = 0$, equation (19) reduces to Henry model equation (20).

$$q_e = \frac{A}{1 + B} C_e \tag{20}$$

where A/(1+B) is the Henry's constant.

3.2.3. Sips model

Recognizing the problem of the continuing increase in the adsorbed amount with an increase in concentration in the Freundlich equation, Sips (1948) proposed equation (21), which is similar in form to the Freundlich equation, but it has a finite limit when the concentration is sufficiently high:

$$q_e = \frac{q_{ms} K_s C_e^{ms}}{1 + K_s C_e^{ms}} \tag{21}$$

where q_{ms}, K_S and *ms* are the Sips maximum adsorption capacity (mg/g), the Sips equilibrium constant $(L/mg)^{ms}$, and the Sips model exponent, respectively. Sips model, my also named as Langmuir-Freundlich model and represented as equation 22.

3.2.4. Langmuir-Freundlich model

The Langmuir-Freundlich equation (22) is given by Sips (1948):

$$q_e = \frac{q_{mLF} K_{LF} C_e^{m_{LF}}}{1 + K_{LF} C_e^{m_{LF}}} \tag{22}$$

where q_{mLF}, K_{LF} and m_{LF} are the Langmuir-Freundlich maximum adsorption capacity (mg/g), the equilibrium constant for a heterogeneous solid and the heterogeneity parameter (lies between 0 and 1), respectively.

(18)

3.2.5. Fritz-Schlunder model

The Fritz-Schlunder model (Fritz and Schlunder, 1974) has proposed a three-parameter empirical expression which can represent a broad field of equilibrium data (equation 23):

$$q_e = \frac{q_{mFS} K_{FS} C_e}{1 + q_{mFS} C_e^{m_{FS}}} \tag{23}$$

where q_{mFS}, K_{FS} and m_{FS} are the Fritz-Schlunder maximum adsorption capacity (mg/g), the Fritz-Schlunder equilibrium constant (L/mg) and the Fritz-Schlunder model exponent, respectively.

3.2.6. Redke-Prausnitz model

The three Redke-Prausnitz models (Radke and Prausnitz, 1972; Costa *et al*., 1986) can be represented as follow (equations 24-27).

$$\frac{1}{q_e} = \frac{1}{KC_e} + \frac{1}{kC_e^{1/P}} \tag{24}$$

$$q_e = \frac{q_{m_{RP1}} K_{RP1} C_e}{(1 + K_{RP1} C_e)^{m_{RP1}}} \quad (25)$$

$$q_e = \frac{q_{m_{RP2}} K_{RP2} C_e}{1 + K_{RP2} C_e^{m_{RP1}}} \quad (26)$$

$$q_e = \frac{q_{m_{RP3}} K_{RP3} C_e^{m_{RP3}}}{1 + K_{RP3} C_e^{m_{RP1}-1}} \quad (27)$$

where q_{mRP1}, q_{mRP2}, and q_{mRP3} are the Redke-Prausnitz maximum adsorption capacities (mg/g), K, K_{RP1}, K_{RP2}, and K_{RP3} are the Redke-Prausnitz equilibrium constants, and P, m_{RP1}, m_{RP2}, and m_{RP3} are the Redke-Prausnitz models exponents.

3.2.7. Tóth model

The Tóth model (Tóth, 2000) is a modification of the Langmuir equation to reduce the error between experimental data and predicted values of equilibrium adsorption data. The application of Tóth equation is best suited to multilayer adsorption similar to BET isotherms which is a special type of Langmuir isotherm and has very restrictive validity (Khan and Ataullah, 1997). The Tóth model is given by the following equation (28).

$$q_e = \frac{q_{m_T} C_e}{(1/K_T + C_e^{m_T})^{1/m_T}} \quad (28)$$

where q_{mT}, K_T and m_T are the Tóth maximum adsorption capacity (mg/g), Tóth equilibrium constant and Tóth model exponent, respectively.

3.2.8. Jossens model

The Jossens isotherm model (Jossens *et al*., 1978; Rudzinski and Everett, 1992; Tripathy *et al*., 2006) is based on a distribution of the energy of interactions adsorbate-adsorbent on adsorption sites. It considers that the activated carbon surface is heterogeneous, with respect to the interactions which it engages with the adsorbate (equation 29).

$$C_e = \frac{q_e}{H} \exp(F q_e^p) \quad (29)$$

where H, F, and P are the parameters of the equation of Jossens. This equation can be reduced to henry's law at low capacities.

3.3. Four-parameter isotherm models

3.3.1. Weber-van Vliet model

Weber and van Vliet (van Vlient *et al*., 1980) have proposed an empirical relation with four parameters to describe equilibrium data (equation 30).

$$C_e = P_1 q_e^{(P_2 q_e^{P_3} + P_4)} \quad (30)$$

where P_1, P_2, P_3 and P_4 are the isotherm parameters.

3.3.2. Baudu model

Baudu (Baudu, 1990) has transformed the Langmuir equation to the following expression (equation 31).

$$q_e = \frac{q_{m0} b_0 C_e^{(1+x+y)}}{1 + b_0 C_e^{(1+x)}} \quad (31)$$

where q_{m0} and b_0 are the Baudu maximum adsorption capacity (mg/g) and the equilibrium constant, respectively, x and y are the Baudu parameters. For lower surface coverage, equation (31) reduces to the Freundlich equation.

3.3.3. Fritz-Schlunder model

The Fritz-Schlunder model (Fritz and Schlunder, 1974) has proposed another four-parameter equation of Langmuir-Freundlich type which can be developed empirically. It is expressed by the equation (32).

$$q_e = \frac{\alpha 1_{mFS} C_e^{\beta 1}}{1 + \alpha 2_{mFS} C_e^{\beta 2}} \quad (32)$$

where $\alpha 1_{mFS}$ and $\alpha 2_{mFS}$ are the Fritz-Schlunder maximum, and $\beta 1$ and $\beta 2$ are the Fritz-Schlunder equilibrium exponents. At high liquid-phase concentrations of the adsorbate, equation (32) reduces to the Freundlich equation. For $\beta 1 = \beta 2 = 1$, Eq. (30) reduces to the Langmuir equation.

3.4. Five-parameter isotherm models

3.4.1. Fritz-Schlunder model

Fritz and Schlunder (Fritz and Schlunder, 1974) have proposed a five-parameter empirical expression which can represent a broad field of equilibrium data (equation 33).

$$q_e = \frac{q_{m_{FSS}} K_1 C_e^{m_1}}{1 + K_2 C_e^{m_2}} \quad (33)$$

where q_{mFSS} is the Fritz-Schlunder maximum adsorption capacity (mg/g) and K_1, K_2, m_1, and m_2 are the Fritz-Schlunder parameters.

The two-parameter models can be readily linearized and hence the parameter values can be easily obtained using the linear least square technique. However, for three and more parameter models, statistical software SPSS version 15.0 based on Windows Vista has been used, which in turn, utilizes the Marquardt-Levenberg optimization procedure. In this optimization procedure, two criteria (sum of squares and parameter convergence) are met to obtain parameter values. The correlation coefficient values are also reported with the output of the result.

3.5. Best-fit isotherm model

To find out the best-fit isotherm model to the experimental equilibrium data, several different error functions have been studied. Using symbol N as the number of experimental data points and P as the number of parameters in the isotherm model, the error functions are applied as following:

3.5.1. Average percentage errors (APE)

The average percentage errors (APE) calculated according to equation (34) indicated the fit between the experimental and predicted values of adsorption capacity used for plotting isotherm curves (Ng *et al*., 2002).

$$\mathrm{APE}(\%) = \frac{100}{N} \times \sum_{i=1}^{N} \left| \frac{q_{e,isotherm} - q_{e,calc}}{q_{e,isotherm}} \right|_i \quad (34)$$

3.5.2. Hybrid fractional error (HYBRID)

The hybrid fractional error function is employed as it compensates for low concentrations by balancing absolute deviation against fractional error and is more reliable than other error functions (Porter *et al*., 1999; Allen *et al*., 2003). The hybrid error is given as equation (35).

$$\mathrm{HYBRID} = \frac{100}{N-P} \times \sum_{i=1}^{N} \left| \frac{q_{e,isotherm} - q_{e,calc}}{q_{e,isotherm}} \right|_i \quad (35)$$

3.5.3. Chi- square error (X^2)

The chi- square error, X^2, (Ho *et al*., 2005) is given as equation (36).

$$X^2 = \sum_{i=1}^{N} \frac{(q_{e,isotherm} - q_{e,calc})^2}{q_{e,isotherm}} \quad (36)$$

3.5.4. Sum of the squares of the errors (ERRSQ)

The sum of the squares of the errors (ERRSQ) (Ng *et al*., 2002) is given by the following equation (37).

$$\mathrm{ERRSQ} = \sum_{i=1}^{N} (q_{e,calc} - q_{e,isotherm})_i^2 \quad (37)$$

3.5.5. Marquardt's percent standard deviation (MPSD)

The Marquart's percentage standard deviation (MPSD) (Ng *et al*., 2002) is given by the following equation (38).

$$\mathrm{MPSD} = 100 \times \sqrt{\frac{1}{N-P} \sum_{i=1}^{N} \left(\frac{q_{e,calc} - q_{e,isotherm}}{q_{e,isotherm}} \right)_i^2} \quad (38)$$

3.5.6. The sum of absolute errors (EABS)

The sum of the absolute errors (EABS) (Ng *et al*., 2002) is given by the following equation (39).

$$\mathrm{EABS} = \sum_{i=1}^{N} \left| q_{e,calc} - q_{e,isotherm} \right|_i \quad (39)$$

3.5.7. The root mean square errors (RMS)

The root mean square errors (RMS) (Ng *et al*., 2002) are given by the following equation (40).

$$\mathrm{RMS} = 100 \times \sqrt{\frac{1}{N} \sum_{i=1}^{N} \left(1 - \frac{q_{e,calc}}{q_{e,isotherm}} \right)^2} \quad (40)$$

3.6. Adsorption kinetics studies

The kinetics of the adsorption describes the rate of MB uptake on RHC which controls the equilibrium time. Four kinetics models, pseudo first-order (Lagergren, 1898), pseudo second-order (Ho *et al*., 2000), Elovich (Zeldowitsch, 1934; Chien and Clayton, 1980; Sparks, 1986), intra-particle diffusion (Weber and Morris, 1963; Srinivasan *et al*., 1988) and film diffusion (Boyd *et al*., 1949) models are used to analyze the sorption data to identify the mechanism of solute adsorption onto sorbents.

3.6.1. Pseudo first-order kinetic model

The Lagergren first-order model (Lagergren, 1898) is the earliest known one describing the adsorption rate based on the adsorption capacity. It is generally expressed as equation (41).

$$\frac{dq_t}{dt} = k_1(q_e - q_t) \quad (41)$$

where, q_e and q_t are the adsorption capacity at equilibrium and at time t, respectively (mg/g), k_1 is the rate constant of pseudo first-order adsorption (L/min). Equation (41) was integrated with the boundary conditions of $t = 0$ to $t = t$ and $q_t = 0$ to $q_t = q_t$ and rearranged to the linear equation (42).

$$\log(q_e - q_t) = \log(q_e) - \frac{k_1}{2.303}t \quad (42)$$

The values of log ($q_e - q_t$) were linearly correlated with t. The plot of log ($q_e - q_t$) versus t should give a linear relationship from which k_1 and predicted q_e can be determined from the slope and intercept of the plot, respectively. The variation in rate should be proportional to the first power of concentration for strict surface adsorption. However, the relationship between initial solute concentration and rate of adsorption will not be linear when pore diffusion limits the adsorption process.

3.6.2. Pseudo second-order kinetic model

The pseudo-second-order model given by Ho *et al*. (2000) as equation (43).

$$\frac{dq_t}{dt} = k_2(q_e - q_t)^2 \quad (43)$$

where k_2 (g/mg min) is the second-order rate constant of adsorption. Integrating equation (44) for the boundary conditions $q = 0$ to $q = q_t$ at $t = 0$ to $t = t$ is simplified as can be rearranged and linearized to obtain:

$$\left(\frac{t}{q_t}\right) = \frac{1}{k_2 q_e^{\,2}} + \frac{1}{q_e}(t) \quad (44)$$

The second-order rate constants were used to calculate the initial sorption rate, h, given by equation (45).

$$h = k_2 q_e^2 \quad (45)$$

If the second-order kinetics is applicable, then the plot of t/q_t versus t should show a linear relationship. Values of k_2 and equilibrium adsorption capacity q_e can be calculated from the intercept and slope of the plots of t/q_t versus t.

3.6.3. Elovich kinetic model

Elovich kinetic equation is another rate equation based on the adsorption capacity, which is generally expressed as equation (46) (Zeldowitsch, 1934; Chien and Clayton, 1980; Sparks, 1986).

$$\frac{dq_t}{dt} = \alpha \exp(-\beta q_t) \quad (46)$$

where α is the initial adsorption rate (mg/g min) and β is the de-sorption constant (g/mg) during any one experiment. It is simplified by assuming $\alpha\beta t >> t$ and by applying the boundary conditions $q_t = 0$ at $t = 0$ and $q_t = q_t$ at $t = t$ equation (46) becomes form as equation (47).

$$q_t = \frac{1}{\beta}\ln(\alpha\beta) + \frac{1}{\beta}\ln(t) \quad (47)$$

plot of q_t versus ln(t) should yield a linear relationship with a slope of ($1/\beta$) and an intercept of ($1/\beta$) × ln($\alpha\beta$). Thus, the constants can be obtained from the slope and the intercept of the straight line.

3.6.4. The intraparticle diffusion model

The possibility of intra-particular diffusion (Weber and Morris, 1963; Srinivasan *et al*., 1988) is explored by using equation (48).

$$q_t = K_{dif} t^{1/2} + C \quad (48)$$

where C is the intercept and K_{dif} is the intra-particle diffusion rate constant. The values of q_t correlated linearly with values of $t^{1/2}$ and the rate constant K_{dif} directly evaluated from the slope of the regression line.

The values of intercept C provide information about the thickness of the boundary layer, the resistance to the external mass transfer increase as the intercept increase.

3.6.5. Film diffusion model

When the transport of the solute molecules from the liquid phase to the solid phase boundary plays a most significant role in adsorption, the liquid film diffusion model (Boyd, 1949) can be applied (equation 49):

$$\ln(1 - F) = -K_{FD}(t) \quad (49)$$

where F and K_{FD} are the fractional attainment of equilibrium ($F = q_t/q_e$), and the film diffusion rate constant, respectively.

4. Results and discussion

4.1. Effect of pH

Since the wastewater of textile industries has a wide range of pH, it is essential to investigate the influence of initial pH of the solution. The effect of pH on the amount of color removal is analyzed over the pH range from 1.0 to 12. The equilibrium time is determined based on several trial experiments carried out for different initial dye concentration. The trial

experiments show that equilibrium time is varied between 150 to 180 min. Thus in the present study 3h of contact time is provided in order to assure that equilibrium is achieved. Figure 2 shows the effect of initial solution pH on the percentage removal of dye at equilibrium conditions. From Figure 2, it is observed that the removal of MB from aqueous solution increase from 66.2 to 99.4% for an increase in pH from 1 to 7.1 and the percentage removal decreased from 99.4 to 77.0% for an increase in pH from 7.1 to 8.5 followed by an increase from 77.0 to 83.2% for increase in pH from 8.5 to 12. Optimum pH value for dye adsorption is observed at pH 7.1, which in agreement with the literature results (El-Sikaily *et al*., 2006b; Hamdaoui, 2006). Low pH (1-6) is unfavorable for methylene blue adsorption by RHC. As pH of the system decrease, the number of negatively charged adsorbent sites decrease and the number of positively charged surface sites increase, which did not favor the adsorption of positively charged dye cations due to electrostatic repulsion. Also, lower adsorption of MB at acidic pH is due to the presence of excess H^+ ions competing with MB cations for the adsorption sites. This, however, did not explain the decrease of dye adsorption at basic pH. These might be another mode of adsorption (ion exchange or chelation for example).

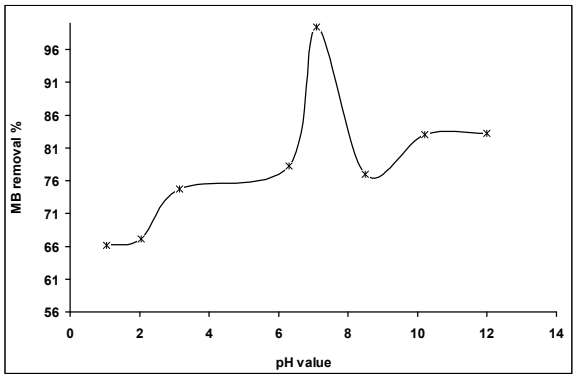

Figure 2. Effect of pH on adsorption of MB (75 mg/L) onto RHC (5.0 g/L) at 25±2°C.

4.2. Effect of contact time

Figure 3 shows the percentage removal of MB at different initial dye concentrations ranging from 68 to 98% at pH 7.1 using 2 g RHC/L of MB solutions of initial concentrations ranged from 25 to 125 mg/L. It can be seen from the figure that the removal of MB increases with increase in time and after 30 min the rate of removal is very low. Most of MB is removed within 60 min and reaches a maximum at 3 h and thereafter remains constant. The optimum time to attain the equilibrium is 3 h. The slow rate of dye adsorption after the first 30 min is probably occurred due to the slow pore diffusion of the solute ion into the bulk of the adsorbent.

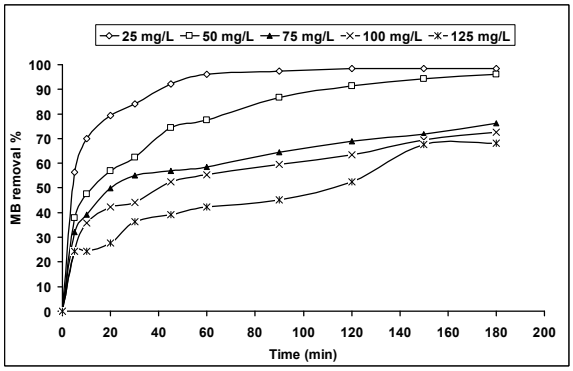

Figure 3. Effect of contact time on the removal of different initial concentrations of MB using RHC (2 g/L) at pH 7.1.

4.3. Effect of initial dye concentration and RHC mass

The influence of the initial concentration of MB in solutions on the rate of adsorption on RHC was studied. The experiment were carried out at adsorbent doses (0.1-0.5 g/100 ml) in the test solution, 25±2°C temperature, pH 7.1 and at different initial concentrations of MB (25, 50, 75, 100 and 125 mg/L) for 3 hrs. Figure 4 shows the plot of equilibrium uptake capacity, q_e (mg/g) and its initial concentration using different doses of RHC. It is observed that the amount of dye adsorbed onto unit weight of sorbent is decreased with increasing of mass concentration. The dye uptake decreased from 85.17 mg/g to 24.87 mg/g for an increase in RHC concentration from 1 g to 5 g/L for MB of concentration 125 mg/L. Whereas the q_e increases from 24.6 to 85.17 mg/g for an increase in initial concentration of MB from 25 to 125 mg/L using 1.0 g/L of RHC. The increase in % color removal is due to the increase in the vacant adsorption sites with increasing biomass thus favoring more dye uptake. The decrease in q_e value may be due to the splitting effect of flux (concentration gradient) between sorbets and sorbent with increasing RHC concentration causing a decrease in amount of MB adsorbed onto unit weight of RHC produces a lower solute concentration is lower. This can be explained on the basis of initial concentration gradient between the solid adsorbent and the bulk liquid. For a fixed volume of dye solution and for a fixed initial dye concentration, the initial concentration gradient between the adsorbent and the

dye solution gets decreased with increasing initial dye concentration. It is likely that the amount of dye adsorbed onto unit weight of adsorbent gets increased with the driving force, i.e. the initial concentration gradient. However in this case for a fixed volume of dye solution and initial dye concentration, the initial concentration gradient between the adsorption vacant sites of the solid adsorbent and the concentration of dye solutions gets decreased with increasing adsorbent mass leading to decrease in q_e value. In the present study, from Figure 4, it can be observed that for all the sorbet mass studied, the concentration in dye solution was in excess to that of the maximum vacant sites available at the surface of the adsorbent. However the q_e value still found to decrease with increasing sorbet mass. This effect may be attributed due to the reduction in overall surface area of the sorbent probably because of aggregation during the sorption (Dönmez *et al*., 1999; Nuhoglu *et al*., 2005).

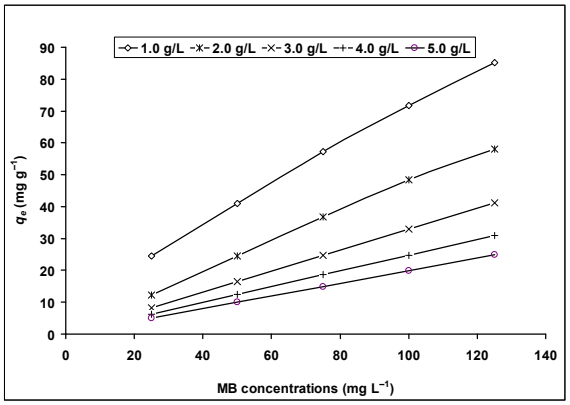

Figure 4. Relation between amounts of MB adsorbed at equilibrium (q_e) and its initial concentration using different doses of RHC.

4.4. Modeling of adsorption isotherms

Several mathematical models are used to describe experimental data of adsorption isotherms. The equilibrium data are modeled with the two-parameter isotherm models including the Langmuir (non-linear), Freundlich, Tempkin, Dubinin-Radushkevich, Harkins-Jura, Halsey, Henderson, Smith and Generalized isotherm. The three-parameter isotherm models including Redlich-Peterson, Sips, Langmuir-Freundlich, Fritz-Schlunder, Radke-Prausnitz, Tóth and Jossens isotherm models were also applied. The four-parameter models including Weber-van Vliet, Fritz-Schlunder, Baudu and the five-parameter model including Fritz-Schlunder have also been studied.

These studies are very important in optimizing the design parameters for any adsorption system and provide sufficient information on the physicochemical data in evaluating the adsorption process as a unit operation. The distributions of solutes between the solid adsorbent and liquid phase are a measure of the position of equilibrium. Equilibrium data should accurately fit into different isotherm models to find a suitable model that can be used for the design process (Ozmihci and Kargi, 2006). The parameters obtained from the different models provide important information on the sorption mechanisms, the surface properties and affinities of the sorbent. Equilibrium data can be expressed by several equations, such as the Langmuir, Freundlich, Koble-Corrigan, Redlich-Peterson, Tempkin, Dubinin-Radushkevich and Generalized isotherm equations and the applicability of isotherm equations is compared by judging the correlation coefficients.

4.4.1. Linear and Non-linear solvation of two parameters models

Table 1 shows the data obtained from isotherm models having two parameters obtained from Linear and Non-linear solvation. The theoretical Langmuir sorption isotherm (Kargi and Ozmichi, 2004) is the most widely used for the adsorption of a pollutant from a liquid solution. It is valid for adsorption of a solute from a liquid solution as monolayer adsorption on specific homogenous sites (a finite number of identical sites) within the adsorbent surface, which are energetically equivalent (Ozmihci and Kargi, 2006; Kargi and Cikla, 2006). Therefore, the Langmuir isotherm model estimates the maximum adsorption capacity produced from complete monolayer coverage on the adsorbent surface. The results obtained from Langmuir model (equations 2 and 3) for the removal of MB onto RHC have correlation coefficients R^2 0.98~1.00 (Table 1) for the linear form (Redlich and Peterson, 1959; Sips, 1948; Fritz and Schlunder, 1974). Figures 5 and 6 show the isotherm plots and the experimental data of Langmuir isotherms whose constants were obtained from equation (3). This figure indicates the applicability of Langmuir isotherm model. The maximum monolayer capacity Q_m obtained from linear and non-linear solvation of Langmuir model is 121.95 and 264.44 mg/g, respectively. The correlation coefficients for non-linear solvation are ranged from R^2 0.926 ~ 0.993 for the different weight, which may indicate that the linear solvation of Langmuir isotherm model may be more applicable than the non-linear solvation.

The Freundlich isotherm model (equation 4) (Freundlich, 1906) is applicable to the adsorption on heterogeneous surfaces with interaction between adsorbed molecules. It is also suggests that sorption energy exponentially decreases on completion of the sorption centers of an adsorbent. Therefore, Freundlich isotherm can be employed to describe the heterogeneous systems. K_F represents the quantity of dye adsorbed onto adsorbent for unit equilibrium concentration. $1/n_F$ is the heterogeneity factor and it is a measure of the deviation from linearity of adsorption. The n_F value indicates the degree of non-linearity between solution concentration and adsorption as

follows: if the value of $n_F = 1$, the adsorption is linear; $n_F < 1$, the adsorption process is chemical; if $n_F > 1$, the adsorption is a favorable physical process (Kargi and Cikla, 2006).

Table 1. Isotherm two parameters models obtained from linear and non-linear solvation.

Isotherm Model	Isotherm Parameters	RHC concentrations				
		1 g/L	2 g/L	3 g/L	4 g/L	5 g/L
Non-linear Langmuir (equation 2)	Q_m (mg/g)	360.71	69.43	264.44	112.45	61.78
	K_a x 10^3	689.80	629.20	142.00	290.70	68.80
	R^2	0.989	0.993	0.972	0.985	0.926
Linear Langmuir (equation 3)	Q_m (mg/g)	95.24	68.49	121.95	88.50	23.75
	K_a x 10^3	573.77	648.89	383.18	407.94	6578.13
	R^2	0.999	0.998	1.000	0.987	0.980
Freundlich	$1/n$	0.27	0.61	0.86	0.77	0.85
	K_F ($mg^{1-1/n}L^{1/n}g^{-1}$)	34.52	24.70	33.33	25.42	33.70
	R^2	0.972	0.989	0.987	0.997	0.928
Tempkin	A_T	14.65	6.59	4.30	7.06	6.57
	B_T	14.00	15.55	23.50	12.00	17.12
	b_T	176.98	159.37	105.41	206.41	144.68
	R^2	0.993	0.999	0.999	0.989	0.995
Harkins-Jura isotherm	A_{HJ}	1.25	0.77	0.15	0.06	0.09
	B_{HJ}	1.65	1.03	0.16	0.10	0.16
	R^2	0.992	0.745	0.877	0.817	0.923
Halsey isotherm	$1/n_H$	0.28	0.48	1.12	1.05	1.20
	K_H	194921.34	733.15	23.44	22.13	21.61
	R^2	0.953	0.938	0.946	0.983	0.957
Henderson isotherm	$1/n_h$	1.07	1.41	1.41	1.48	1.49
	K_h	0.02	0.05	0.02	0.02	0.01
	R^2	0.852	0.780	0.830	0.900	0.921
Smith isotherm	W_{bs}	21.32	10.32	11.32	7.53	3.58
	W_s	6.66	2.66	6.66	6.98	19.32
	R^2	0.930	0.878	0.780	0.857	0.933
Generalized isotherm	N_b	0.34	0.54	0.96	0.83	1.22
	K_G	6.72	10.04	7.08	9.61	5.85
	R^2	0.982	0.991	0.990	0.998	0.985

isotherm can be employed to describe the heterogeneous systems. K_F represents the quantity of dye adsorbed onto adsorbent for unit equilibrium concentration. $1/n_F$ is the heterogeneity factor and it is a measure of the deviation from linearity of adsorption. The n_F value indicates the degree of non-linearity between solution concentration and adsorption as follows: if the value of $n_F = 1$, the adsorption is linear; $n_F < 1$, the adsorption process is chemical; if $n_F > 1$, the adsorption is a favorable physical process (Kargi and Cikla, 2006).

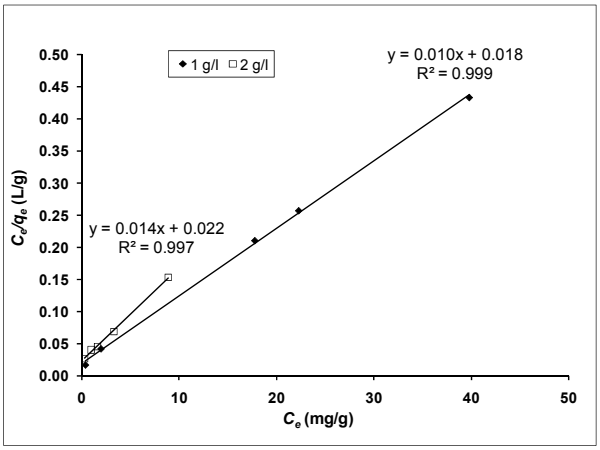

Figure 5. Linear Langmuir model for adsorption of MB over 1 and 2 g/L of RHC

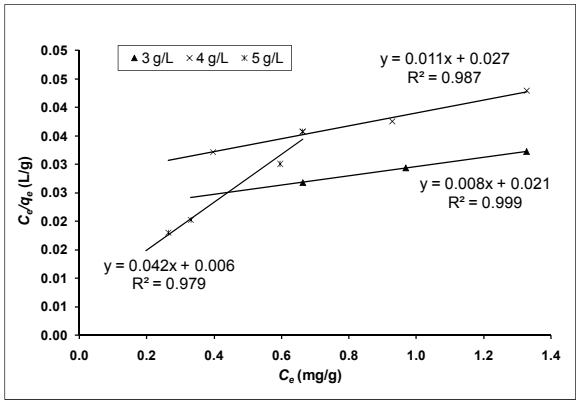

Figure 6. Linear Langmuir model for adsorption of MB over 3, 4 and 5 g/L of RHC

Figure 7 represents the plot of $\log(q_e)$ versus $\log(C_e)$ with the intercept value of $\log K_F$ and the slope of $1/n_F$. The correlation coefficients, $R^2 > 0.928 \sim 0.997$, obtained from Freundlich model is comparable to that obtained from the non-linear solvation of Langmuir model (Table 1). This result indicates that the experimental data fitted Freundlich model less than Langmuir and the $n_F > 1$, indicating that adsorption of MB onto RHC is a favorable physical process (Kargi and Cikla, 2006). The Harkins–Jura adsorption isotherm can be expressed (Harkins and Jura, 1944) as

equation (13), which can be solved by plot of $1/q_e^2$ versus log C_e as shown in Figure 8. Harkins–Jura model accounts to multilayer adsorption and can be explained with the existence of a heterogeneous pore distribution. Isotherm constants and correlation coefficients are ranged from R^2 0.745~0.992 for the different weights (Table 1). This may indicates that the Harkins-Jura model is less applicable than the Langmuir and Freundlich models.

Halsey (Halsey, 1948) and Henderson (Henderson, 1952) adsorption isotherm can be given as, equations (14) and (15), respectively. These equations are suitable for multilayer adsorption. Especially, the fitting of these equations can be heteroporous solids (Rosen, 1978). Plot of ln q_e versus ln C_e Halsey and ln[−ln(1−C_e)] versus ln q_e Halsey and Henderson adsor ption isotherms are given in Figures 9 and 10, respectively. Isotherm constants and correlation coefficients are summarized in Table 1. Halsey shows correlation coefficients ranged between R^2 0.938 ~ 0.983, while Henderson shows R^2 0.780 ~ 0.921. The results obtained for Halsey and Henderson show that both models are less applicable to the adsorption of MB onto RHC.

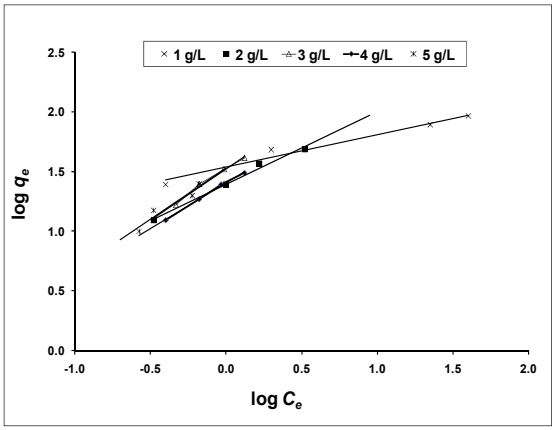

Figure 7. Linear Freundlich model of adsorption of MB over 1, 2, 3, 4 and 5 g/L of RHC.

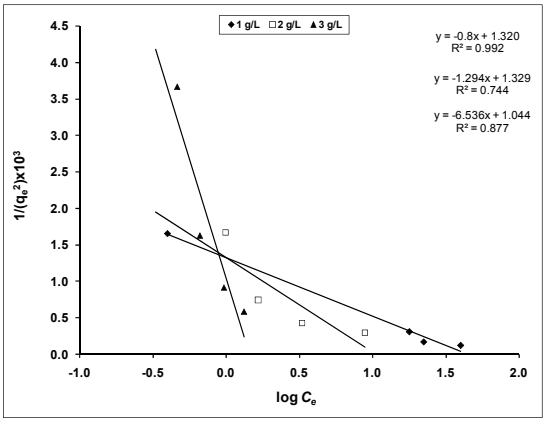

Figure 8. Linear Harkins–Jura model of adsorption of MB over 1, 2, and 3 g/L of RHC.

Smith model (equation 16) is useful in describing the sorption isotherm of biological materials such as starch and cellulose and is suitable for multilayer adsorption and the fitting of Smith equations can be seen in heteroporous solids. Smith model can be solved by plot of q_e versus ln(1-C_e) as shown in Figure 11. Smith models adequately represented the sorption isotherms throughout the entire range of water activity. However, the Henderson and the Smith equations were less successful for describing the isotherms of MB onto RHC because the two models gave smaller R^2 values.

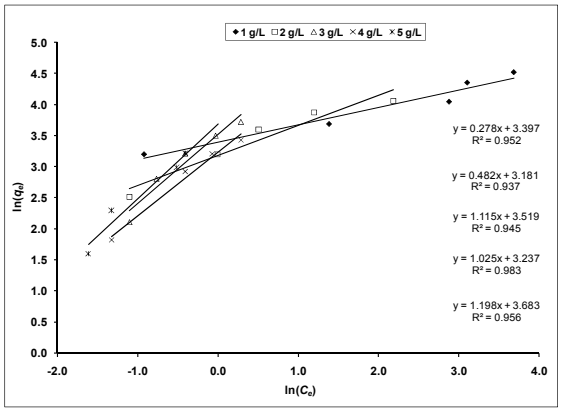

Figure 9. Linear Halsey model of adsorption of MB over 1 - 5 g/L of RHC.

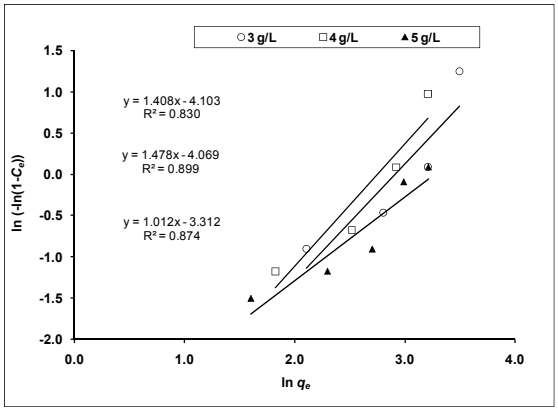

Figure 10. Linear Henderson model of adsorption of MB over 3 - 5 g/L of RHC.

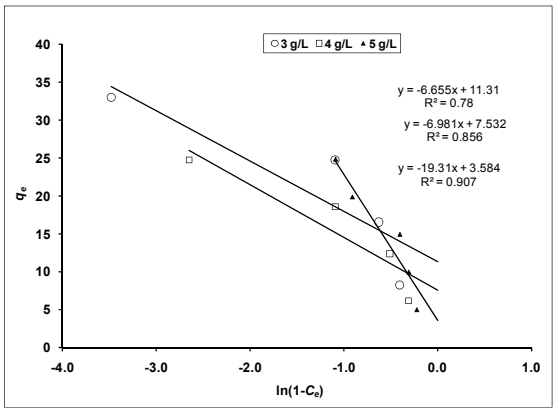

Figure 11. Linear Smith model of adsorption of MB over 3 - 5 g/L of RHC.

A linear form of the generalized isotherm equation (Lagergren, 1898) is given by equation (17) and can be solved linearly by the plot of $\log[(Q_m/q_e)-1]$ versus $\log C_e$; the intercept gave $\log K_G$ and the slope gave N_b constants. Parameters related to each isotherm were determined by using linear regression analysis and the square of the correlation coefficients (R^2) have been calculated. A list of the parameters obtained together with R^2 values is given in Table 1. A comparison of the experimental isotherms with the adsorption isotherm models showed that the generalized equation and Langmuir represent the best fit of experimental data as compared to the other isotherm equations ($R^2 > 0.980$). Based on the isotherm data of two parameter model can be seen that the obtained data fit well only the Langmuir and generalized isotherm models. The maximum monolayer capacity obtained for MB adsorption on RHC was 121.95 mg/g.

Tempkin isotherm model (Tempkin, 1940; Khan *et al*., 1997) assumes that the heat of adsorption of all the molecules in the layer decreases linearly with coverage due to adsorbate-adsorbent interactions as well as the adsorption is characterized by a uniform distribution of maximum binding energy (Aharoni and Ungarish, 1977). The derivation of the Tempkin isotherm assumes that the fall in the heat of sorption is linear rather than logarithmic, as implied in the Freundlich equation. The Tempkin isotherm has commonly been applied in the form equation (7) (Tempkin, 1940; Jossens, 1978; Rudzinski and Everett, 1992; Tripathy *et al*., 2006): The Tempkin isotherm equation (7) can be expressed in its linear form equation (8) (van Vlient *et al*., 1980; Baudu, 1990). Figure 12 shows the adsorption data according to the linear form of the Tempkin isotherm equation (8) and value of constants and coefficients are given in Table 1. The correlation coefficients obtained are $R^2 > 0.989$, which indicates that the Tempkin isotherm fit well the equilibrium data obtained for the adsorption of MB onto RHC. Non-linear solvation of Tempkin isotherm model gave similar data.

4.4.2. Solvation of three parameters models

Koble-Corrigan model equation (18) (Costa *et al*., 1986) are solved using SPSS version 15.0 computer program and reported in Table 2. The correlation coefficients obtained were 0.989, 0.994, 0.994, 991 and 0.943 for adsorption of MB onto RHC doses 1, 2, 3, 4 and 5 g/L, respectively, indicating that Koble-Corrigan model fit well to the experimental data obtained for adsorption of MB onto RHC except for 5 g concentration of RHC. However, the value of *b* was ranged between 0.38 and 4.28, which indicates the combination between heterogeneous and homogeneous adsorption of MB onto RHC.

Redlich and Peterson (Redlich and Petersen (1959)) non-linear equation (19) is solved using nonlinear regression analysis and the three isotherm constants *A*, *B* and *g* are reported in Table 2. The correlation coefficients obtained were low for 1 and 5 g concentration of RHC indicating that the Redlich-Peterson isotherm can be consider as less applicability than Langmuir and Freundlich isotherm models for data obtained from adsorption of MB onto RHC.

Combining Langmuir and Freundlich isotherms give the Sips isotherm and expected to describe heterogeneous surfaces much better (equation 21) (Sips, 1948). At low sorbate concentration, the Sips isotherm assumes the form of the Freundlich model, while at high concentrations it predicts a constant, monolayer sorption behavior similar to that of the Langmuir isotherm. The Sips isotherm gave the good fit at low concentration as Langmuir isotherm while at higher concentration it give lower fit as Freundlich model which may be proved the data obtained from the two parameters models Langmuir and Freundlich (Table 1 and 2). According to Sips model, the monolayer adsorption capacity value was 132.61 mg/g, which is closed to that obtained for linear Langmuir 121.95 mg/g.

Langmuir-Freundlich isotherm (equation 22) (Sips, 1948) model is similar to Sips isotherm model and has the same information. The application of Langmuir-Freundlich model gave R^2 close to that obtained by Sips model (Table 2). The m_{LF} values are almost 1, which indicates that it is more applicable as Langmuir isotherm than Freundlich isotherm model. The q_{mLF} was 376.44 mg/g which is higher than that obtained by non-linear solvation of Langmuir model 360.71 mg/g (Table 1).

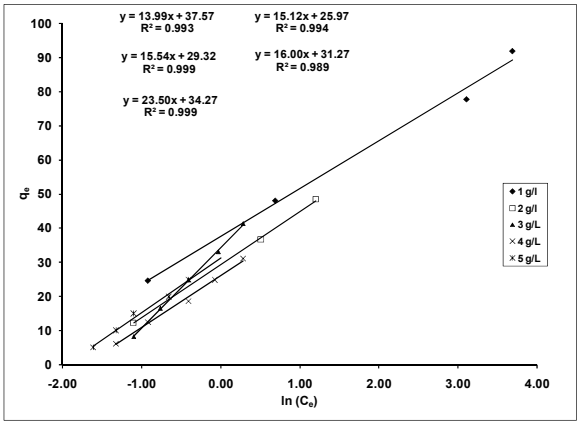

Figure 12. Linear Tempkin isotherm model of adsorption of MB over 1 - 5 g/L of RHC.

Dubinin-Radushkevich (D-R) isotherm model (Radushkevich, 1949; Dubinin, 1960, 1965) dose not assume a homogeneous surface or constant sorption potential. It was applied to estimate the porosity apparent free energy and the characteristic of adsorption and it has commonly been applied in the form equation (9) and its linear form can be shown in equation (10).

Figure 13 shows the plot of ln q_e versus ε^2 of the experimental data for the adsorption of MB onto RHC.

The slope gives K (mol^2 (kJ^2)$^{-1}$) and the intercept yields the adsorption capacity, Q_m (mg/g). The mean free energy of adsorption (E), defined as the free energy change when one mole of ion is transferred from infinity in solution to the surface of the sorbent. E was calculated from the K value using the equation (12) (Ho *et al*., 2005).

Calculated D-R constants for the adsorption of MB on RHC are shown in Table 2; the values of correlation coefficients $R^2 > 0.988$ which indicating that the D-R fit well the experimental data in comparable with the Langmuir and Tempkin isotherm models. The maximum capacity Q_m obtained using D-R isotherm model for adsorption of MB is 30.04 mmole/g on RHC dose of 4.0 g/L (Table 2). The values of E calculated using equation (12) are 0.33, 0.39, 0.30, 0.29 and 0.30 kJ/mol. The typical range of bonding energy for ion-exchange mechanisms is 8-16 kJ/mol, indicating that physic-sorption plays a significant role in the adsorption process of MB ion onto RHC.

Jossens *et al*. (1978) incorporated the features of the Langmuir and Freundlich isotherms into a single equation (29) and presented a general isotherm equation in agreement with equation (19) proposed by Redlich and Petersen (1959). The non-linear solvation of Eq. 29 gave high correlation coefficient $R^2 > 0.982$ indicting that Jossens isotherm model is comparable with Langmuir, Tempkin and D-R isotherm models but more applicable than Redlich-Peterson isotherm model.

Non-linear solvation of the three parameters Fritz-Schlunder isotherm model (equation 23) (Fritz and Schlunder, 1974) shows high accuracy at low concentration of RHC giving $R^2 > 0.991$.

The abilities of the three-parameter Radke–Prausnitz (four models) isotherm models equation (24-27) (Radke and Prausnitz, 1972; Costa *et al*., 1986) at the equilibrium adsorption data were examined. Linear solvation of Radke–Prausnitz 1 by plot of $1/q_e$ versus $1/C_e$ gave fit well for the experimental data at lower concentrations of RHC (Figure 14). Table 2 shows the isotherms parameters obtained using the non-linear fitting analysis for Radke–Prausnitz 2-4 isotherm models. All four equations are applicable at low concentration of RHC and represent lower fit at higher concentration of RHC (Table 2). The maximum adsorption capacities obtained from the four equations are 87.72, 110.13, 99.21 and 159.74 mg/g.

Tóth isotherm (equation 28) (Tóth, 2000; Khan *et al*., 1997) is Langmuir-based isotherm and considers a continuous distribution of site affinities. Non-linear solvation of three parameters Tóth isotherm model shows 166.07 mg/g maximum capacity for the adsorption of MB on 1 g of RHC (Table 2). The correlation coefficients show high accuracy at low concentration of RHC which is similar to most studied models above. However Tóth isotherm is less accuracy than Langmuir isotherm models for the adsorption of MB onto RHC.

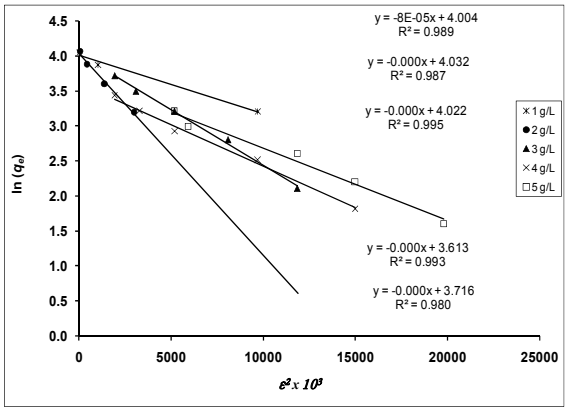

Figure 13. Linear Dubinin-Radushkevich isotherm model of adsorption of MB over 1 - 5 g/L of RHC.

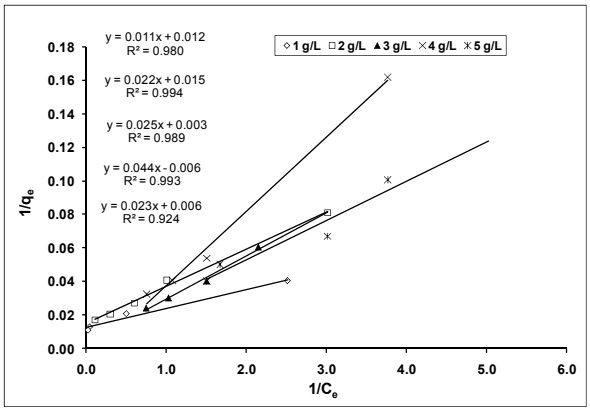

Figure 14. Linear Radke-Prausnitz 1 isotherm model of adsorption of MB over 1 - 5 g/L of RHC.

4.4.3. Solvation of four and five parameters models

Non-linear solvation of the four parameters Weber-van Vliet isotherm model (equation 30) (van Vlient *et al*., 1980) shows high accuracy only at RHC concentration of 3 and 4 g/L (Table 3). Similar data obtained from linear solvation of Weber-van Vliet isotherm model (Figure 15).

Four parameters Baudu isotherm model (equation 31) (Baudu, 1990) is a modification of Langmuir isotherm model. Non-linear solvation of Baudu isotherm model gave maximum capacity 96.51 mg/g for the adsorption of MB by RHC (Table 3). The correlation coefficients obtained for Baudu isotherm model (R^2) are 0.990, 0.996, 0.997, 0.994 and 0.978 for 1-5 g/L, respectively.

Table 2. Three parameters isotherm models.

Isotherm Model	Isotherm Parameter	Rice husk activated carbon concentrations				
		1.0 g/L	**2.0** g/L	**3.0** g/L	**4.0** g/L	**5.0** g/L
Koble-Corrigan	a (L/g)	48.21	44.54	106.64	61.49	150.00
	b (L/mg)	0.38	0.67	2.06	1.35	4.28
	n	0.46	1.10	2.04	1.54	1.81
	R^2	0.989	0.994	0.994	0.991	0.943
Redlich-Peterson	A (L/g)	150.00	43.69	37.66	32.76	37.71
	B (L/mg)^g	3.44	0.63	0.14	0.29	0.07
	g	0.82	1.00	1.00	1.00	1.00
	R^2	0.886	0.993	0.972	0.985	0.926
Sips	q_{mS} (mg/g)	132.61	66.43	51.76	45.51	44.37
	K_S (L/mg)^g	0.38	0.67	2.06	1.35	5.81
	m_S	0.46	1.10	2.03	1.53	3.35
	R^2	0.989	0.994	0.994	0.995	0.958
Langmuir-Freundlich	q_{mLF} (mg/g)	376.44	69.43	264.03	112.80	279.72
	K_{LF} (L/mg)	0.10	0.62	0.14	0.29	0.14
	m_{LF}	0.99	1.00	1.00	1.00	1.00
	R^2	0.994	0.993	0.972	0.985	0.925
Dubinin-Radushkevich	Q_m (mol/kg)	2.89	1.93	22.10	30.04	28.37
	$K \times 10^6$ (mol/kJ)^2	4.60	3.30	5.40	6.00	5.70
	E (kJ/mol)	0.33	0.39	0.30	0.29	0.30
	R^2	0.989	0.991	0.996	0.993	0.988
Jossens isotherm	H	3.17	10.19	1.78	1.82	1.82
	F	14.76	191.80	-3.48	-2.66	-2.96
	P	-16.60	-52.36	-0.05	0.00	0.00
	R^2	0.982	0.991	0.990	0.998	0.995
Fritz-Schlunder	q_{mFS} (mg/g)	3.52	0.39	3.87	2.02	0.45
	K_{FS}	47.83	93.21	41.77	37.49	110.81
	m_{FS}	0.83	1.12	0.25	0.26	0.10
	R^2	0.995	0.995	0.991	0.979	0.970
Radke-Prausnitz 1	K	87.72	45.05	38.61	32.62	42.74
	k	74.40	59.35	283.67	100.00	160.55
	$1/P$	0.034	0.100	0.001	0.001	0.001
	R^2	0.986	0.968	0.986	0.993	0.925
Radke-Prausnitz 2	q_{mRP1} (mg/g)	85.44	110.13	16.34	21.36	44.10
	K_{RP1}	2.30	0.35	2.39	1.63	0.82
	m_{RP1}	0.76	1.26	0.14	0.33	0.10
	R^2	0.999	0.996	0.969	0.983	0.961
Radke-Prausnitz 3	q_{mRP2} (mg/g)	87.83	99.21	46.30	39.98	51.32
	K_{RP2}	0.52	0.39	3.009	1.74	1.82
	m_{RP2}	0.83	1.13	0.28	0.32	0.10
	R^2	0.995	0.995	0.992	0.983	0.926
Radke-Prausnitz 4	q_{mRP3} (mg/g)	159.74	53.37	44.38	33.51	37.75
	K_{RP3}	0.30	1.03	3.066	3.12	14.89
	m_{RP3}	0.17	0.11	0.10	0.10	0.10
	R^2	0.995	0.986	0.994	0.984	0.926
Tóth isotherm	q_{mT} (mg/g)	166.07	63.64	44.86	30.98	32.88
	$1/K_T$	0.52	2.19	5.286	9.65	0.11
	m_T	0.28	1.32	6.73	18.84	31.32
	R^2	0.991	0.995	0.979	0.989	0.965

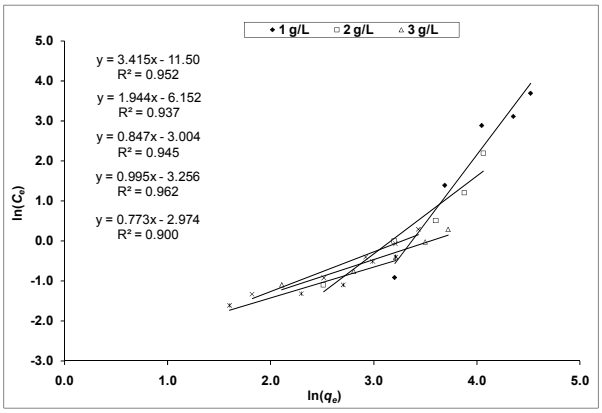

Figure 15. Linear Weber-van Vliet isotherm model of adsorption of MB over 1 - 5 g/L of RHC.

Four parameters Fritz-Schlunder isotherm model (equation 32) (Fritz and Schlunder, 1974) was used and found to represent their adsorbate–adsorbent system well. Thus, it may be concluded that for the same system of MB/activated carbon systems, different isotherms have been used and Fritz-Schlunder isotherm model gave the high accuracy as Langmuir and Generalize isotherm models. The correlation coefficients are 0.992, 0.997, 0.999, 0.996 and 0.974 obtained for different concentrations of RHC of 1-5 g/L, respectively, via non-linear solvation of equation 32 (Table 3). However, the predicted q_e using the parameter obtained from Fritz-Schlunder isotherm model are very closed to that obtained from experimental results (Figure 16).

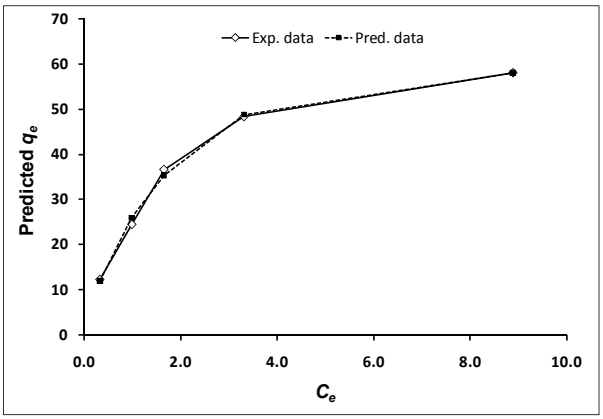

Figure 16. Comparison between Exp. q_e values and q_e predicted values by solvation of Fritz-Schlunder isotherm model for removal of MB by RHC.

Table 3: Four and five parameters isotherm models

Isotherm Model	Isotherm Parameter	Rice husk activated carbon concentrations				
		1.0 g/L	2.0 g/L	3.0 g/L	4.0 g/L	5.0 g/L
Weber-van Vliet isotherm	P_1	1.008	1.228	1.096	1.010	1.011
	P_2	100.45	-66.77	-47.254	40.68	-4.75
	P_3	0.01	-0.01	-0.01	0.01	-0.19
	P_4	-103.00	64.78	45.884	-42.245	2.48
	R^2	0.957	0.971	0.999	0.994	0.966
Baudu isotherm	q_{m0} (mg/g)	29.10	96.51	41.23	42.76	21.56
	b_0	33.67	0.37	4.818	1.57	-1.04
	x	-1.00	0.12	-3.03	-2.63	-3.35
	y	0.32	-0.13	1.090	1.311	0.77
	R^2	0.990	0.996	0.997	0.994	0.978
Fritz-Schlunder	α_{1mFS} (mg/g)(mg/L)$^{-\beta 1}$	88.01	29.16	232.30	165.66	38.34
	α_{2FS} (mg/L)$^{-\beta 2}$	1.42	0.12	5.819	5.36	4.96
	β_{1FS}	0.74	0.79	2.26	2.10	1.15
	β_{2FS}	0.62	1.23	1.816	1.719	86.91
	R^2	0.992	0.997	0.999	0.996	0.974
Fritz-Schlunder	q_{mFS}	38.00	5.74	5.92	5.08	20.34
	K_1	38.00	5.74	5.9216	5.08	20.34
	m_1	3.01	0.90	0.60	0.66	2.44
	K_2	35.19	0.26	0.028	0.007	14.16
	m_2	2.79	1.13	-3.354	-3.569	2.31
	R^2	0.997	0.996	0.999	0.998	0.952

Also non-linear solvation of the five parameters Fritz-Schlunder isotherm model (equation 33) (Fritz and Schlunder, 1974) gave similar results (Table 3). This may be proved the applicability of Fritz-Schlunder isotherm models to the adsorption of MB onto RHC.

4.5. Error functions Studies for Best-fit isotherm model

The best-fit isotherm model for the experimental data was studied by several different error functions. The applied error functions are the Average percentage errors (APE) equation (34) (Ng *et al*., 2002), Hybrid fractional error (HYBRID) equation (35) (Porter *et al*., 1999; Allen *et al*., 2003), Chi-square error (X^2) equation (36) (Ho *et al*., 2005), Sum of the squares of the errors (ERRSQ) equation (37) (Ng *et al*., 2002), Marquardt's percent standard deviation (MPSD) equation (38) (Ng *et al*., 2002), The sum of absolute errors (EABS), equation (39) (Ng *et al*., 2002), The root mean square errors (RMS) equation (40) (Ng *et al*., 2002). The data obtained from different error

functions are summarized in Table 4. From the obtained data, the lowest accuracy isotherm models are Weber-van Vliet isotherm, Jossens isotherm, Harkins-Jura isotherm and smith isotherm models. The best fit isotherm models are Tempkin, Koble-Corrigan, Langmuir isotherm, and Langmuir-Freundlich isotherm models. However, the error functions studied gave variable results for each isotherm model and the comparison between the isotherm models should be focused for each error functions separately. For example, the Chi-square error (X^2) equation (36), and the sum of absolute errors (EABS), equation (39) show that all the isotherm models are comparable and applicable to the experimental data except Harkins-Jura isotherm, Jossens isotherm, and Weber-van Vliet isotherm models, while the other, gave more two or three isotherm models cannot be applied to the experimental data.

Table 4: Represent the best-fit isotherm model to the experimental equilibrium data by several different errors functions.

Isotherm Model	Eq. No.	APE%	X^2	Hybrid	ERRSQ	MPSD	EABS	RMS
Non-linear Langmuir	2	9.93	0.28	10.21	7.96	15.38	2.11	15.38
Linear-Langmuir	3	5.26	0.28	9.26	6.47	7.57	2.13	7.57
Freundlich	5	12.06	0.36	12.02	5.72	22.28	1.82	22.28
Tempkin	8	5.07	0.09	5.07	2.62	8.11	1.08	8.11
Dubinin-Radushkevich	11	12.85	0.90	26.40	28.32	21.14	3.31	21.14
Harkins-Jura isotherm	13	27.44	3.04	28.63	49.62	39.10	7.38	38.28
Halsey isotherm	14	11.34	0.41	11.34	17.96	13.18	3.24	13.18
Henderson isotherm	15	16.94	0.77	19.55	21.63	20.14	3.46	18.75
Smith isotherm	16	22.77	0.82	22.77	9.97	34.04	2.49	34.04
Generalized isotherm	17	8.84	0.24	8.84	7.77	13.84	1.90	13.84
Koble-Corrigan	18	6.14	0.10	6.41	3.56	9.41	1.29	9.21
Redlich-Peterson	19	8.57	0.20	8.96	5.93	15.28	1.73	14.94
Sips	21	13.43	0.62	14.04	8.81	26.74	1.99	26.16
Langmuir-Freundlich	22	9.94	0.26	10.85	6.40	17.42	1.85	16.68
Fritz-Schlunder 3P	23	7.93	0.14	8.29	2.20	13.61	1.27	13.31
Redke-Prausnitz 1	24	9.28	0.23	9.70	8.04	16.11	2.00	15.76
Redke-Prausnitz 2	25	8.55	0.19	8.94	5.93	13.71	1.73	13.41
Redke-Prausnitz 3	26	9.09	0.20	9.50	3.88	16.08	1.66	15.73
Redke-Prausnitz 4	27	7.69	0.14	8.04	2.65	13.73	1.36	13.43
Toth isotherm	28	7.15	0.12	7.48	2.43	11.88	1.24	11.62
Jossens isotherm	29	26.93	4.92	29.37	72.84	40.83	6.90	39.09
Weber-van Vliet	30	92.47	21.26	101.28	862.30	97.48	25.96	93.14
Baudu isotherm	31	7.05	0.16	7.72	3.02	12.03	1.14	11.49
Fritz-Schlunder 4P	32	5.37	0.09	5.88	2.20	9.14	1.03	8.74
Fritz-Schlunder 5P	33	3.76	0.04	4.32	1.03	6.78	0.74	6.33

4.6. Adsorption kinetic studies

Several models were used to examine the rate-controlling of the adsorption process such as chemical reaction, diffusion control and mass transfer. Since the kinetic parameters are helpful for the prediction of adsorption rate and give important information for designing and modeling the adsorption processes, the kinetics of the adsorption of MB onto RHC was investigated for selecting optimum operating conditions for a full-scale batch process. Therefore, pseudo first-order (Ho *et al*., 2002), pseudo second-order (Zeldowitsch, 1934), Elovich (Chien and Clayton, 1980; Sparks, 1980; Weber and Morris, 1963) and intraparticle diffusion (Srinivasan *et al*., 1980; Boyd *et al*., 1949) kinetic models were applied for the adsorption of MB on RHC and the conformity between experimental data and the model-predicted values was expressed by the correlation coefficients (R^2).

4.6.1. Pseudo first-order equation

The rate constant of adsorption is determined from the Lagergren pseudo-first-order model (Ho *et al*., 2000), the earliest known equation describing the adsorption rate based on the adsorption capacity, which is commonly expressed as equation (41).

Table 5. Comparison of the first- and second-order adsorption rate constants and calculated and experimental q_e values for different initial MB and RHC concentrations.

Parameter			First-order kinetic model			Second-order kinetic model			
RHC (g/L)	MB (mg/L)	q_e (exp.)	q_e (calc.)	k_1 x 10^3	R^2	q_e (calc.)	k_2 x 10^3	h	R^2
1.0	25	24.60	15.46	54.58	0.964	25.38	8.62	5552	1.000
	50	48.01	34.06	*23.2603*	0.990	52.08	1.16	3146	0.998
	75	57.21	36.93	14.97	0.953	60.24	0.82	2992	0.978
	100	77.70	47.29	13.36	0.843	81.30	0.61	4016	0.979
	125	91.81	94.12	22.34	0.714	111.11	0.46	5711	0.993
2.0	25	12.33	1.10	26.25	0.845	12.41	74.24	11429	1.000
	50	24.50	6.00	27.87	0.828	25.00	13.79	8621	1.000
	75	36.67	25.88	28.56	0.996	40.00	1.73	2764	0.997
	100	48.34	24.82	17.50	0.993	51.02	1.76	4572	0.998
	125	58.05	44.49	15.89	0.975	64.94	0.52	2203	0.987
3.0	25	8.22	0.38	24.64	0.951	8.24	225.67	15337	1.000
	50	16.51	1.55	26.48	0.722	16.67	42.76	11876	1.000
	75	24.78	11.88	29.02	0.954	25.97	4.68	3161	0.998
	100	33.01	10.70	32.01	0.918	34.01	6.63	7669	1.000
	125	41.22	9.18	30.40	0.792	42.02	8.61	15198	1.000
4.0	25	6.18	0.30	29.25	0.859	6.20	305.39	11723	1.000
	50	12.40	0.72	20.73	0.804	12.45	116.18	18018	1.000
	75	18.58	4.60	43.76	0.909	18.90	22.17	7924	1.000
	100	24.77	3.46	19.81	0.744	25.13	16.57	10460	1.000
	125	30.92	3.87	20.50	0.815	31.35	15.90	15625	1.000
5.0	25	4.96	0.24	35.24	0.977	4.97	465.38	11507	1.000
	50	9.95	0.45	37.31	0.937	9.97	257.29	25575	1.000
	75	14.93	5.42	133.11	0.950	14.95	46.20	10326	1.000
	100	19.88	1.64	25.10	0.773	18.76	53.30	18762	1.000
	125	24.87	7.64	46.29	0.921	24.92	101.20	62846	1.000

Figure 17 represents plot the values of $\log(q_e - q_t)$ versus t and the Lagergren parameters, k_1 and q_e, can be calculated from the slope and intercept, respectively. If the calculated q_e dose not equal the experimental q_e then the reaction is not likely to be first order reaction even this plot has high correlation coefficient with the experimental data (Kargi and Cikla, 2006). However, the relationship between initial dye concentration and rate of adsorption will not be linear when pore diffusion limits the adsorption process. Figure 17 shows that the data does not fit the Lagergren model as the R^2 values are low and the calculated q_e values are too low compared with experimental q_e for all adsorption data (Table 5), which indicates that the adsorption of MB onto RHC are not a first-order reaction.

4.6.2. Pseudo second-order equation

The adsorption kinetic may be described by a pseudo-second-order (Ho *et al*., 2000; Zeldowitsch, 1934). The differential equation is generally given as equation (43) and (44). The initial adsorption rate, h, the equilibrium adsorption capacity, q_e, and the second-order constants k_2 (g/mg min) can be determined experimentally from the slope and intercept, respectively, of plot t/q_t versus t (Figure 18). Calculated correlations are equal to unity for second-order kinetics model; therefore the adsorption kinetics could well be approximated more favorably by second-order kinetic model for MB. The values of k_2, q_e, h and correlation coefficients, R^2, of dye under different conditions were calculated from these plots (Table 5).

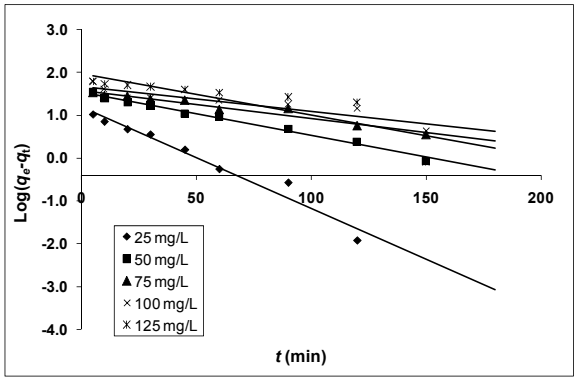

Figure 17. Plot the values of $\log(q_e - q_t)$ versus t for removal of MB (25 – 125 mg/L) by RHC (1.0 g/L).

The calculated q_e values are mainly equal to the experimental data, which further indicates that the MB-RHC adsorption system obeys the pseudo-second-order kinetic model for the entire sorption period. The values of initial adsorption rate (h) that represent the rate of initial adsorption, is practically increased with the increase in initial dye concentrations, while the pseudo-second-order rate constant (k_2) decreased with increasing of initial dye concentration from 25 to 125 mg/L (Table 5).

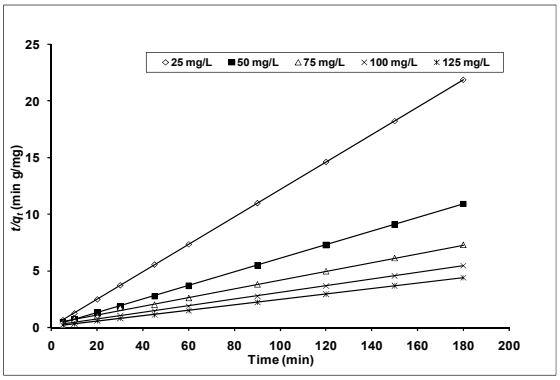

Figure 18. Plot t/q_t versus t of the pseudo-second-order model for removal of MB (25-125 mg/L) by RHC (5.0 g/L).

4.6.3. Elovich kinetic equation

Elovich equation is a rate equation based on the adsorption capacity usually given by the equations (46) and (47) (Zeldowitsch, 1934; Chien and Clayton, 1980; Sparks, 1986). Figure 19 shows plot of q_t versus ln(t) and the Elovich constants were calculated from the slope ($1/\beta$) and intercept ($1/\beta$)ln($\alpha\beta$) of the straight lines and reported in Table 6. The correlation coefficients R^2 are wavy and ranged between 0.896 and 0.985 without definite role, which reflects the inapplicability of this model to the experimental data obtained for the adsorption of MB on RHC.

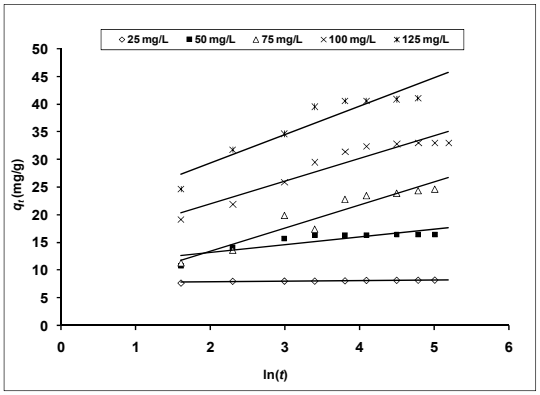

Figure 19. Plot q_t versus ln(t) of the pseudo-second-order model for removal of MB (25-125 mg/L) by RHC (5.0 g/L).

4.6.4. Intraparticle diffusion model

Adsorption mechanism for any dye removal by adsorption process on a solid phase material may be assumed to involve the following four steps: (i) migration of dye from its solution to the surface of the solid phase (bulk diffusion); (ii) diffusion of dye through the boundary layer to the surface of the solid phase (film diffusion); (iii) transport of dye from the solid phase surface to its particles interior pores (pore diffusion or intraparticle diffusion); (iv) adsorption of dye at an active site on the solid phase surface (Chemical reaction such as ion-exchange, complexation and chelation). The dye adsorption is usually controlled by either the intraparticle or the liquid-phase mass transport rates (Kargi and Cikla, 2006). If the experiment is a batch system with rapid stirring, there is a possibility that intraparticle diffusion is the rate controlling step (Hamdaoui, 2006). This possibility was tested in terms of a graphical relationship between q_t and the square root of time, $t^{1/2}$, according to the intraparticle diffusion model proposed by Weber and Morris (1963). Since the MB is probably transported from its aqueous solution to the RHC by intraparticle diffusion, so the intraparticle diffusion is another kinetic model should be used to study the rate-limiting step for MB adsorption onto RHC. The root of time dependence is commonly expressed by the equations (62) and (63) (Rudzinski and Everett, 1992).

If the intraparticle diffusion is involved in the adsorption process, then the plot of q_t versus $t^{1/2}$ would result in a linear relationship, and the intraparticle diffusion would be the controlling step if this line passed through the origin (Nuhoglu *et al*., 2005). The shape of Figure 20 confirms straight lines not passed through the origin with correlation coefficients ranged from low to high value without definite meaning, which is indicative of some degree of boundary layer control and this further shows that the intraparticle

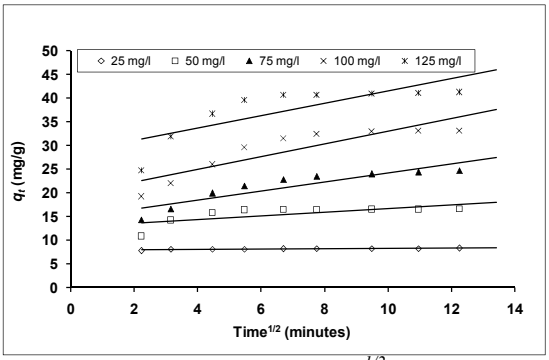

Figure 20. The plot of q_t versus $t^{1/2}$ of interaparticle diffusion model for removal of MB (25-125 mg/L) by RHC (5 g/L).

diffusion is not only the rate controlling step for the adsorption of the MB on RHC, but also other processes may control the rate of adsorption. The C value was

found to increase with increase of initial dye concentration, which indicated increase of the thickness of the boundary layer and decrease of the chance of the external mass transfer and hence increase of the chance of internal mass transfer. On the other hand, the *C* value decreased with increase of carbon dose, which reflect decrease of the thickness of the boundary layer and hence increase of the chance of the external mass transfer.

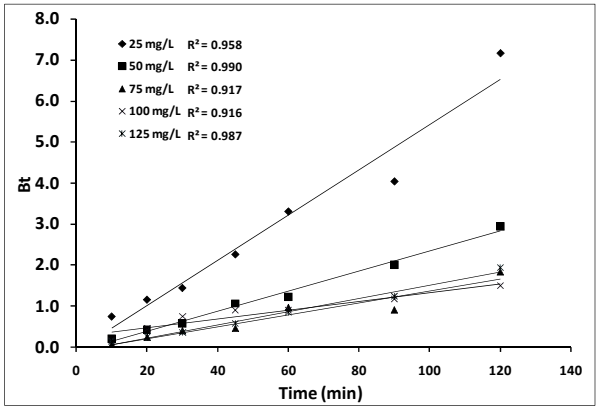

Figure 21. Plot of *Bt* versus *t* of intraparticle diffusion kinetic model for removal of MB (25-125 mg/L) by RHC (1.0 g/L).

The intraparticle diffusion rate constant, K_{dif}, was in the range of 0.04-0.82 mg g^{-1} $min^{-1/2}$ and it increase with increase of initial dye concentration and decrease of RHC dose.

Plots of *Bt* versus *t* are also shown in Figure 21, which are near the straight lines and show that the intraparticle diffusion is not the only rate controlling step and some fraction of the sorption occurs through external diffusion (film diffusion) because the plots do not pass through the origin and the R^2 is slightly low.

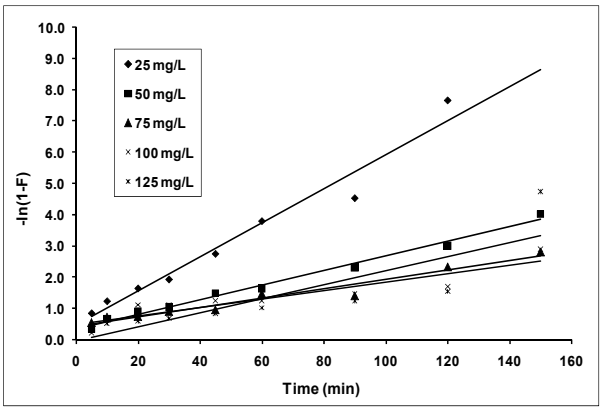

Figure 22. Plot of – ln(1-*F*) versus t of Film diffusion model for removal of MB (25-125 mg/L) onto RHC (1 g/L).

Table 6: Comparison of the kinetic models Elovich, interaparticle diffusion and film diffusion.

RHC (g/L)	MB (mg/L)	Elovich			interaparticle diffusion 2			Film diffusion		
		β	α	R^2	K_{dif}	C	R^2	K_{FD}	C	R^2
1.0	25	0.32	7.79E+01	0.952	0.17	1.08	0.986	0.05	0.46	0.964
	50	0.10	9.36E+00	0.991	0.29	1.07	0.985	0.02	0.34	0.990
	75	0.08	6.02E+00	0.950	0.30	1.07	0.984	0.01	0.44	0.953
	100	0.07	1.19E+01	0.942	0.25	1.31	0.965	0.01	0.50	0.842
	125	0.08	2.09E+01	0.946	0.32	0.04	0.980	0.02	0.03	0.714
2.0	25	3.36	2.28E+15	0.893	0.02	1.04	0.885	0.03	2.41	0.849
	50	0.37	2.41E+02	0.813	0.10	1.19	0.863	0.04	1.47	0.911
	75	0.14	8.71E+00	0.954	0.25	1.04	0.960	0.03	0.22	0.996
	100	0.14	3.77E+01	0.966	0.20	1.26	0.973	0.02	0.56	0.994
	125	0.08	5.78E+00	0.962	0.40	0.87	0.951	0.02	0.27	0.975
3.0	25	7.72	4.01E+24	0.856	0.02	0.88	0.849	0.03	3.12	0.938
	50	0.71	2.29E+03	0.722	0.12	0.98	0.885	0.04	2.05	0.836
	75	0.24	1.44E+01	0.911	0.16	1.07	0.934	0.03	0.73	0.955
	100	0.24	1.16E+02	0.914	0.17	1.36	0.800	0.06	0.37	0.988
	125	0.20	2.16E+02	0.881	0.14	1.19	0.917	0.04	1.43	0.086
4.0	25	14.08	3.03E+34	0.949	0.01	0.77	0.949	0.03	2.75	0.783
	50	2.53	1.64E+11	0.733	0.03	1.03	0.718	0.03	2.80	0.983
	75	0.53	3.95E+02	0.776	0.13	1.02	0.734	0.04	1.58	0.841
	100	0.40	5.16E+02	0.795	0.08	1.33	0.750	0.03	1.79	0.831
	125	0.46	3.30E+04	0.766	0.12	1.15	0.760	0.03	1.83	0.907
5.0	25	16.45	1.30E+32	0.956	0.01	0.67	0.954	0.03	3.05	0.990
	50	0.87	4.01E+05	0.708	0.02	0.96	0.732	0.05	2.73	0.857
	75	1.90	1.14E+10	0.759	0.04	1.10	0.745	0.03	2.90	0.795
	100	5.84	2.88E+22	0.739	0.07	1.17	0.687	0.05	1.84	0.927
	125	0.40	5.18E+02	0.809	0.12	1.15	0.771	0.04	1.47	0.898

4.6.5. Film diffusion model

In order to assess the nature of the diffusion process responsible for adsorption of MB on RHC, attempts were made to calculate the coefficients of the process. Straight lines were obtained when $-\ln(1-F)$ was plotted against time, t (Figure 22) which did not pass through the origins (Boyd, 1949). This indicates that film diffusion is not limiting step of the overall adsorption process kinetics. Figure 21 on the other hand, indicates that straight lines were obtained on plotting Bt versus time, t which nearly passes through the origins. This shows that intraparticle diffusion and film diffusion may be share in the rate controlling step.

5. Conclusion

Kinetic and equilibrium studies were reported for the adsorption of Methylene Blue from aqueous solutions onto activated carbon developed from rice husk carbon can be effectively used as an adsorbent for the removal of dye. Experimental data indicated that the adsorption capacity was dependent of operating variables such as adsorbent mass, pH, contact time and initial dye concentration. The adsorption process was strongly pH-dependent. The straight lines in plot of t/q_t versus t showed good agreement of experimental data with the second-order kinetic model for different initial dye concentrations and activated carbon doses. The linear correlation coefficients obtained from this model were equal to unity under all concentrations used and the values of equilibrium sorption capacity were in the best agreement with q_e experimental data, which confirm the applicability of the pseudo-second-order model. It was also observed that intraparticle diffusion and film diffusion models are involved in the rate determining step of the adsorption process. Elovich model does not fit the experimental data judging to the low correlation coefficients obtained by this model. Henderson isotherm models showed the poorest two parameters isotherm models while Langmuir and Generalized isotherm models showed the best fit models. Redlich-Peterson isotherm model showed the poorest fitting of the three parameters isotherm models to the experimental data, while the other tested three parameters models were expressed good agreement with the experimental data obtained. The maximum sorption capacity was 376.44 mg/g at room temperature and pH value 1.5 by Langmuir-Freundlich model.

References

Abdelwahab, O., El Nemr, A., El-Sikaily, A., Khaled. A.: 2005, Use of rice husk for adsorption of direct dyes from aqueous solution: A case study of Direct F. Scarlet. *Egyptian Journal for Aquatic Research,* 31(1): 1-12.

Aharoni, C., Ungarish, M.: 1977, Kinetics of activated chemisorption. Part 2. Theoretical models. *Journal Chemical Society, Faraday Trans* 73: 456-464.

Aharoni, C., Sparks, D.L.: 1991, Kinetics of Soil Chemical Reactions – A Theoretical Treatment, in Sparks DL and Suarez DL (Eds). Rate of Soil Chemical Processes, Soil Science Society of America, Madison, WI. 1-18.

Ajmal, N., Rao, R.A.K., Anwar, S., Ahmad, J., Ahmad, R.: 2003, Adsorption study on rice husk: removal of Cd(II) from waste water. *Bioresource Technology* 86, 147-149.

Akkaya, G., Ozer, A.: 2005, Adsorption of acid red 274 (AR 274) on Dicranella varia: determination of equilibrium and kinetic model parameters. *Process Biochemistry* 40(11): 3559-3568.

Allen, S.J., Gan, Q., Matthews, R., Johnson, P.A.: 2003, Comparison of optimized isotherm models for basic dye adsrption by kudzu. *Bioresource Technology* 88: 143-152.

Baudu, M.: 1990, Étude des interactions solute-fibres de charbon actif. Application et regeneration, Ph.D. Thesis, Université de Renners I.

Bishnoi, N.R., Bajaj, M., Sharma, N., Gupta, A.: 2004, Adsorption of Cr(VI) on activated rice husk carbon and activated alumina. *Bioresource Technology* 91: 305-307.

Boyd, G.E., Adamson, A.M., Myers, L.S.: 1949, The exchange adsorption of ions from aqueous solutions by organic zeolites. *Journal American Chemical Society* 69: 2836.

Chien, S.H., Clayton, W.R.: 1980, Application of Elovich equation to the kinetics of phosphate release and sorption on soils. *Soil Science Society American Journal* 44, 265-268.

Costa, E., Calleja, G., Marijuan, L., Cabra, L.: 1986, Kinetics of adsorption of phenol and *p*-nitrophenol on activatedcarbon. In: A.I. Liapis, editor, *Fundamentals of adsorption*, New York: *American Institute of Chemical Engineers* 195-198.

Doğan, M., Alkan, M., Onganer, Y.: 2000, Adsorption of methylene blue from aqueous solution onto perlite. *Water Air and Soil Pollution* 120: 229-249.

Dönmez, G.C., Aksu, Z., Özturk, A.: 1999, A comparative study on heavy metal biosorption characteristics of some algae. *Process Biochemistry* 34: 885-892.

Dubinin, M.M.: 1960, The potential theory of adsorption of gases and vapors for adsorbents with energetically non-uniform surface. *Chemical Review* 60: 235-266.

Dubinin, M.M.: 1965, Modern state of the theory of volume filling of micropore adsorbents during adsorption of gases and steams on carbon adsorbents. *Zhurnal Fizicheskoi Khimii* 39: 1305-1317.

El Nemr, A., El-Sikaily, A., Khaled, A., Abdelwahab, O.: 2007, Removal of toxic chromium (VI) from aqueous solution by activated carbon developed

from *Casuarina Equisetifolia*, *Chemistry and Ecology* 23(2): 119-129.

El-Sikaily, A., El Nemr, A., Khaled, A., Abdelwahab, O.: 2006a, Removal of Basic Dye (Methylene Blue) from Simulated Textile Dye Effluent by Activated Carbon Developed from Rice Husk. International Conference on Aquatic Resources: Needs and Benefits NIOF, 18-21st September 2006 Alexandria, Egypt, Page 159.

El-Sikaily, A., Khaled, A., El Nemr, A., Abdelwahab, O.: 2006b, Removal of methylene blue from aqueous solution by marine green alga *Ulva lactuca*, *Chemistry and Ecology* 22: 149-157.

Ertugay, M.F., Certel, M., Gürses, A.: 2000, Moisture adsorption isotherms of Tarhana at 25°C and 35°C and the investigation of fitness of various isotherm equations to moisture sorption data of Tarhana. *Journal Science Food and Agricalture* 80: 2001-2004.

Freundlich, H.M.F.: 1906, Über die adsorption in lösungen. *Zeitschrift für Physikalische Chemie (Leipzig)* 57A: 385-470.

Fritz, W., Schlunder, E.U.: 1974, Simultaneous adsorption equilibria of organic solutes in dilute aqueous solution on activated carbon. *Chemical Engineering Science*. 29: 1279-1282.

Govindararo, N.M.H.: 1980, Utilization of rice husk: a preliminary analysis. *Journal Science Industrial Research*, 39: 495-515.

Halsey, G.D.: 1948, Physical adsorption in non-uniform surfaces. *Journal Chemical Physics* 16: 931-945.

Halsey, G.D.: 1952, The role of surface heterogeneity. *Advanced Catalysis* 4: 259-269 (1952).

Hamdaoui, O.: 2006, Batch study of liquid-phase adsorption of methylene blue using cedar sawdust and crushed brick. *Journal Hazardous Materials* B135: 264-273.

Hamdaoui, O., Naffrechoux, E., Sptil, J., Fachinger. C.: 2005, Ultrasonic desorption of *p*-chlorophenol from granular activated carbon. *Chemistry Engineering Journal* 106: 153-161.

Harkins, W., Jura, G.: 1944, Surfaces of solids XIII A vapor adsorption method for the determination of the area of a solid without the assumption of a molecular area, and the areas occupied by nitrogen and other molecules on the surface of a solid. *Journal American Chemical Society* 66: 1366-1371.

Henderson, S.M.: 1952, A basic concept of equilibrium moisture. *Agriculture Engineering* 33(1): 29-31.

Ho, Y.S., Chiu, W.T., Wang, C.C.: 2005, Regression analysis for the sorption isotherms of basic dyes on sugarcane dust. *Bioresource Technology*. 96, 1285–1291.

Ho, Y.S., McKay, G., Wase, D.A.J., Foster, C.F.: 2000, Study of the sorption of divalent metal ions on to peat. *Adsorption Science and Technology* 18: 639-650.

Jossens, L., Prausnitz, J.M., Fritz, E.U., Myers, A.L.: 1978, Thermodynamics of multi-solute adsorption from dilute aqueous solutions. *Chemical Engineering Science* 33: 1097-1106.

Kargi, F., Ozmichi, S.: 2004, Biosorption performance of powdered activated sludge for removal of different dyestuffs. *Enzyme Microbial Technology* 35: 267-271.

Kargi, F., Cikla, S.: 2006, Biosorption of zinc(II) ions onto powdered waste sludge (PWS): kinetics and isotherms. *Enzyme Microbial Technology* 38: 705-710.

Kavitha, D., Namasivayam, C.: 2007, Experimental and kinetic studies on methylene blue adsorption by coir pith carbon. *Bioresource Technology* 98: 14-21.

Khan, A.H., Ataullah, R., Al-Haddad, A.: 1997, Equilibrium adsorption studies of some aromatic pollutants from dilute aqueous solutions on activated carbon at different temperatures. *Journal Colloidal Interference Science* 194: 154-165.

Kinniburgh, D.G.: 1986, General purpose adsorption isotherms. *Environmental Science and Technology* 20: 895-904.

Kundu, S., Gupta, A.K.: 2006, Investigation on the adsorption efficiency of iron oxide coated cement (IOCC) towards As (V)-Kinetics, equilibrium and thermodynamic studies. *Colloids Surface A: Physicochemical Engineering Aspects* 273: 121-128.

Lagergren, S.: 1898, Zur theorie der sogenannten adsorption geloster stoffe. Kungliga Svenska Vetenskapsakademiens. *Handlingar* 24, 1-39.

Langmuir, I.: 1916, The constitution and fundamental properties of solids and liquids. *Journal American Chemical Society* 38: 2221-2295.

Longhinotti, E., Pozza, F., Furlan, L., Sanchez, M.D.N.D., Klug, M., Laranjeira, M.C.M., Favere, V.T.: 1998, Adsorption of anionic dyes on the biopolymer chitin. *Journal Brazilian Chemical Society* 9: 435-440.

Nakbanpote, W., Thiravetyan, P., Kalambaheti, C.: 2000, Preconcentration of gold by rice husk ash. *Minerals Engineering*, 13: 391-400.

Ng, J.C.Y., Cheung, W.H., McKay, G.: 2002, Equilibrium studies of the sorption of Cu(II) ions onto chitosan. *Journal Colloidal Interference Science* 255: 64-74.

Nuhoglu, Y., Malkoc, E., Gürses, A., Canpolat, N.: 2005, The removal of Cu(II) from aqueous solutions by *Ulothrix zonata*. *Bioresource Technology* 85: 331-333.

Ozmihci, S., Kargi, F.: 2006, Utilization of powdered waste sludge (PWS) for removal of textile dyestuffs from wastewater by adsorption. *Journal Environmental Management* 81: 307-314.

Pearce, C.I., Lioyd, J.R., Guthrie, J.T.: 2003, The removal of color from textile wastewater using whole bacterial cells: a review. *Dyes Pigments* 58: 179-196.

Porter, J.F., McKay, G., Choy, K.H.: 1999, The prediction of sorption from a binary mixture of acidic des using single-and mixed-isotherm variants of the ideal adsorbed solute theory. *Chemical Engineering Science* 54: 5863-5885.

Proctor, A., Palaniappans, S.: 1989, Soy oil lutein adsorption by rice hull ash. *Journal of the American Oil Chemists Society,* 66: 1618-1621.

Proctor, A., Palaniappans, S.: 1990, Adsorption of soy oil free fatty acids by rice hull ash. *Journal of the American Oil Chemists Society,* 67: 15-17.

Radke, C.J., Prausnitz, J.M.: 1972, Adsorption of organic solutes from dilute aqueous solution on activated carbon. *International Engineering Chemical Foundation* 11: 445-451.

Radushkevich, L.V.: 1949, Potential theory of sorption and structure of carbons. *Zhurnal Fizicheskoi Khimii* 23: 1410-1420.

Redlich, O., Peterson, D.L.: 1959, A useful adsorption isotherm. *Journal Physical Chemistry* 63: 1024-1026.

Rosen, M.J.: 1978, Surfactants and Interfacial Phenomena, John Willey, New York. 32–76.

Rudzinski, W., Everett, D.: 1992, Adsorption of Gases on Heterogeneous Surfaces, Academic Press, New York.

Sips, R.: 1948, On the structure of a catalyst surface. *Journal Chemistry Physical* 16: 490-495.

Smith, S.E.: 1947, The sorption of water vapour by high polymers. *Journal American Chemical Society* 69: 646.

Sparks, D.L.: 1986, Kinetics of reaction in Pure and Mixed Systems, in Soil Physical Chemistry. CRC Press, Boca Raton.

Srinivasan, K., Balasubramanian, N., Ramakrishan, T.V.: 1988, Studies on chromium removal by rice husk carbon. *Indian Journal of Environtal Health* 30: 376-387.

Tempkin, M.J., Pyzhev, V.: 1940, *Acta Physiochim, URSS* 12: 217-222.

Tóth, J.: 2000, Calculation of the BET-compatible surface area from any type I isotherms measured above the critical temperature. *Journal Colloidal Interference. Science* 225: 378-383.

Tripathy, S.S., Bersillon, J.-L., Gopal, K.: 2006, Removal of fluoride from drinking water by adsorption onto alum-impregnated activated alumina. *Separation Purification Technology* 50: 310-317.

Vadivelan, V., Vasanth Kumar, K.: 2005, Equilibrium, kinetics, mechanism, and process design for the sorption of methylene blue onto rice husk. *Journal Colloidal International Science,* 286: 90-100.

van Vlient, B.M., Weber, W.J., Hozumi, H.: 1980, Modeling and prediction of specific compound adsorption by activated carbon and synthetic adsorbents. *Water Research* 14: 1719-1817.

Vasanth Kumar, K., Sivanesan, S.: 2007, Sorption isotherm for safranin onto rice husk: Comparison of linear and non-linear methods. *Dyes and Pigments* 72: 130-133.

Wang, X.S., Qin, Y.: 2005, Equilibrium sorption isotherms for of Cu^{2+} on rice bran. *Process Biochemistry*. 40: 677-680.

Weber, W.J., Morris, J.C.: 1963, Kinetics of adsorption on carbon from solution. *Journal Sanit. Engineering Division. American Society Civil Engineering* 89: 31-60.

Zeldowitsch, J.: 1934, Über den mechanismus der katalytischen oxidation von CO and MnO_2. *Acta Physicochim. URSS* 1: 364-449.